Global and Planetary Change 133 (2015) 35–48

Contents lists available at ScienceDirect

Global and Planetary Change

journal homepage: www.elsevier.com/locate/gloplacha

Coccolithophore variability from the Shackleton Site (IODP Site U1385) through MIS 16-10

P. Maiorano [a,*], M. Marino [a], B. Balestra [b], J.-A. Flores [c], D.A. Hodell [d], T. Rodrigues [e,f]

[a] Dipartimento di Scienze della Terra e Geoambientali, Università degli Studi di Bari Aldo Moro, Bari, Italy
[b] Institute of Marine Sciences (IMS), University of California, Santa Cruz, USA
[c] Departamento de Geología, Grupo de Geociencias Oceánicas (GGO), Universidad de Salamanca, Salamanca, Spain
[d] Godwin Laboratory for Palaeoclimate Research, Department of Earth Sciences, University of Cambridge, Cambridge, UK
[e] Divisão de Geologia e Georecursos Marinhos, Instituto Português do Mar e da Atmosfera (IPMA), Avenida de Brasília 6, 1449-006 Lisboa, Portugal
[f] CCMAR Associated Laboratory, University of the Algarve, Campus de Gambelas, 8005-139 Faro, Portugal

ARTICLE INFO

Article history:
Received 11 March 2015
Received in revised form 10 June 2015
Accepted 29 July 2015
Available online 31 July 2015

Keywords:
Coccolithophores
Iberian margin
Mid-Pleistocene
Paleoproductivity
Paleoclimate
Orbital-millenial scale variability

ABSTRACT

Coccolithophore assemblages have been investigated at Integrated Ocean Drilling Program Site U1385, on the western Iberian margin, through Marine Isotope Stage (MIS) 16 to 10, between the end of the Mid-Pleistocene Transition and the Mid-Brunhes interval, with the aim to reconstruct orbital and millennial-scale surface water modifications. Assemblage variations are interpreted in terms of paleoclimate and paleoproductivity proxies. The pattern of C_{37} alkenones is also presented as an additional indicator of primary paleoproductivity. The overall proxies are compared with the available benthic and planktonic $\delta^{18}O$ records and Ca/Ti profile. A new benthic and planktonic $\delta^{13}C$ dataset is also shown. The coccolithophore abundance mirrors the Ca/Ti pattern indicating that coccolith-derived carbonate is the dominant contributor to carbonate production in the studied interval. The distinct increase in the coccolithophore abundance, as well as in the accumulation rate, occurring at the MIS 14/13 transition, reflects the beginning of the worldwide-scale mid-Brunhes blooming of *Gephyrocapsa caribbeanica* and triggers the increase in carbonate production imprinted on the Ca/Ti profile. Interglacials are marked by enhanced abundances of the coccolithophore warm water group (wwt group) that also displays high frequency variability related to precessional/insolation forcing. Warmest surface water conditions are recorded during MIS 15, suggesting an intensified contribution of the subtropical AzC, essentially during MIS 15.5 and 15.1. Reduced productivity in these intervals is in agreement with a major influence of nutrient-poor and less ventilated subtropical waters. On the other hand, productive and mixed surface water conditions can be inferred during MIS 13 in agreement with other North Atlantic records. A long lasting period of warm, stratified and oligotrophic waters is inferred during MIS 11.3, indicating a continuous and more persistent influence of subtropical waters at the site location. Glacial phases are marked by increases of *Coccolithus pelagicus* ssp. *pelagicus* and of *Gephyrocapsa margereli–Gephyrocapsa muellerae*. The pattern of *C. pelagicus* ssp. *pelagicus* during MIS 16 is in agreement with a southern position of the Polar Front at the end of the Mid-Pleistocene Transition with respect to younger counterparts, whereas the pattern of the wwt group during MIS 14 attests the influence of subtropical water during this weak glacial. Throughout the interval, short-lived increases of *C. pelagicus* ssp. *pelagicus*, *G. margereli–G. muellerae* > 4 μm and of reworked taxa are concomitant to decreases of coccolithophore productivity and heavier values of planktonic $\delta^{18}O$, testifying the occurrence of abrupt cold episodes related to North Hemisphere millennial-scale climate oscillations.

1. Introduction

Coccolithophore assemblages have been analyzed at the Integrated Ocean Drilling Program (IODP) Site U1385 (Expedition 339 Scientists, 2013), through Marine Isotope Stage (MIS) 16 to 10 with the aim to investigate surface water modifications and related climate variability. The site is located on the southwestern Iberian margin, an area which represents a focal region for investigating past climate variability. It is in fact sensitive to record low latitude wind-driven processes such as dust transport, upwelling and precipitation (Tzedakis et al., 2009; Hodell et al., 2013b) as well as ocean climate variability comparable to Northern and Southern Hemisphere ice cores (Shackleton et al., 2000, 2004; Vautravers and Shackleton, 2006; Martrat et al., 2007; Margari et al., 2010; Hodell et al., 2013b). In particular abrupt cold excursions, i.e., stadial events (Dansgaard et al., 1993) or Heinrich ice-rafting events (HE) (Heinrich, 1988), have provided excellent documentations of

* Corresponding author.
E-mail address: patrizia.maiorano@uniba.it (P. Maiorano).

http://dx.doi.org/10.1016/j.gloplacha.2015.07.009
0921-8181/

Pleistocene millennial-scale climate variability over the past five climate cycles (e.g. Lebreiro et al., 1996; Bard et al., 2000; Pailler and Bard, 2002; de Abreu et al., 2003; Moreno et al., 2002; Sánchez Goñi et al., 2008; Naughton et al., 2009). Data from the last 45 kyr, highlight that the presence of the Polar Front along the Iberian margin was restricted to Heinrich events (Eynaud et al., 2009). During these events, freshwater discharges into the North Atlantic led to a weakened or shutdown of the Atlantic Meridional Overturning Circulation (AMOC) (Maslin et al., 1995; Vidal et al., 1997; Zahn et al., 1997). In the present study we focus on an older time interval, between 693 and 339 ka, which includes the end of the Mid-Pleistocene Transition (MPT) (Mudelsee and Schulz, 1997) and the beginning of the Mid-Brunhes interval (MB) (Jansen et al., 1986; Barker et al., 2006), in order to detect surface water variations at orbital and millennial-scale during a crucial time of pronounced change in the Earth's climate system (Clark et al., 2006; Mudelsee and Schulz, 1997). It is a period including the transition from the predominant obliquity-dominated cycles to predominant eccentricity dominated cycle of 100 kyr (Berger and Jansen, 1994), although the exact timing and mechanism of the onset of the "100 kyr" regime is still under debate. At the end of the MPT larger ice sheet volume developed (Clark et al., 2006; Bintanja and van de Wal, 2008) and the climate state evolved toward generally colder conditions. In this context, MIS 16 represents the first prolonged glacial following the MPT (Clark et al., 2006), a period of modifications of surface water conditions in the subpolar North Atlantic, during which, at about 660 to 610 ka, a northward migration of the Arctic Front (AF) occurred (Wright and Flower, 2002; Naafs et al., 2011). At the same time the onset of Heinrich layers first appears in the central North Atlantic (Hodell et al., 2008; Naafs et al., 2011), sustaining that changes in the volume and dynamics of Northern Hemisphere ice sheets were an important process for the MPT. The interval straddling MIS 15 to 13 is a prolonged period without a deep glacial, characterized by weak interglacial conditions (Lang and Wolff, 2011), although a particular relative strength of MIS 15 has been recorded from Asian record (Prokopenko et al., 2001; Lang and Wolff, 2011). Through the MB, a shift toward more intense interglacial conditions developed after MIS 13 (EPICA community members, 2004; Jouzel et al., 2007; Lang and Wolff, 2011). MIS 11 is in fact considered the first strong interglacial through the MB. It also represents the longest-lasting warm period of the last 1.0 Ma (McManus et al., 1999; Hodell et al., 2000; Jouzel et al., 2007; Rodrigues et al., 2011; Milker et al., 2013), during which the sea level has been suggested to be up to 20 m above the current level (Hearty et al., 1999; Kindler and Hearty, 2000) or close to the Holocene high-stand (Rohling et al., 2009; Bowen, 2010). MIS 11 follows the largest amplitude transition (Termination V) of the last 500 kyr (Oppo et al., 1998; Rodrigues et al., 2011), at the end of MIS 12 known to be the strongest glacial of the last 800 kyr (Lang and Wolff, 2011). At low and high latitude the MB is accompanied by large accumulation of neritic and pelagic carbonate (Howard and Prell, 1994; Howard, 1997; Hodell et al., 2000) and overall poor carbonate preservation (Crowley, 1985; Droxler et al., 1988, 1997; Wu et al., 1991; Bassinot et al., 1994; Droxler and Farrell, 2000; Hodell et al., 2000). During this interval a typical feature among the coccolithophore assemblage is the dominance of the genus *Gephyrocapsa* (Bollmann et al., 1998; Baumann and Freitag, 2004) that has been suggested as a possible cause of the enhanced pelagic carbonate production (Barker et al., 2006).

Through the investigated interval evidences of millennial-scale climate variability are also documented. Specifically, North Atlantic deep-sea cores (McManus et al., 1999; Hodell et al., 2008; Ji et al., 2009; Stein et al., 2009; Alonso-Garcia et al., 2011; Channell et al., 2012) highlight that this period has been punctuated by anomalous occurrences of ice-rafted detritus (IRD) recorded within the IRD belt of Ruddiman (1977) and reflecting North Atlantic ice sheet instability (Dansgaard et al., 1993). Abrupt cold events have been also documented on the western Iberian margin, well beyond the Ruddiman IRD belt, from MIS 15/14 transition up to MIS 9 and referred to Heinrich-type (H-type), based on prominent Sea Surface Temperature (SST) shifts and increases in lithic concentration (Voelker et al., 2010; Rodrigues et al., 2011), attesting high climate variability mainly during MIS 12 and MIS 10. Recent coccolithophore data from western Iberian deep-sea records (Amore et al., 2012; Palumbo et al., 2013; Marino et al., 2014) have focused on climate signals through the interval between MIS 13 to MIS 9. In the area, coccolithophore variations have been related to surface water dynamics linked to ocean–atmosphere settings and specifically to the Azores High (AH)/Icelandic Low (IL) System migration both on glacial/interglacial and precessional-timescale (Amore et al., 2012). With regards to the interglacials a strong influence of the Azores Current has been suggested during MIS 11c (Amore et al., 2012; Marino et al., 2014). In addition, the high climate variability documented across the MB interval during glacials (Stein et al., 2009; Rodrigues et al., 2011; Voelker et al., 2010), appears also well sustained by coccolithophore evidences through the MB. Abrupt abundance variations of specific taxa, as well as rapid fluctuations of reworked specimens observed during glacials MIS 12 and 10, seem to be valuable proxies for recording millennial-scale climate variability (Amore et al., 2012; Palumbo et al, 2013; Marino et al., 2014) as also previously documented for the last glacial cycle (Colmenero-Hidalgo et al, 2004; Incarbona et al., 2010), whereas their identification in older intervals has not been tested yet. On the other hand, data on the occurrence or absence of intra–interglacial instability in the last 800 kyr are rather limited and deserve further investigations (Tzedakis et al., 2009). Differences among individual interglacials in terms of their intensity, duration and climate forcing across the MB transition are also under debate (Yin and Berger, 2012; Candy and McClymont, 2013).

In this framework we have investigated glacial and interglacial climate variability at Site U1385 as deduced by coccolithophore variations. The site was selected since it was recently drilled with the aim to provide a marine reference section of Pleistocene millennial-scale climate variability and to develop an unambiguous marine–ice–terrestrial correlation (Hodell et al., 2013a). It contains a complete record from the Holocene to 1.43 Ma that can be correlated unambiguously to the LR04 benthic $\delta^{18}O$ stack of Lisiecki and Raymo, 2005 (Hodell et al., 2013a; Hodell et al., in this issue). In addition, based on sediment properties, both strong precessional signal and fine-scale millennial variations have been already documented (Hodell et al., 2013a). A good correlation between Ca/Ti profile and the Greenland ice core $\delta^{18}O$ record for the last 120 kyr has been observed. In the area, variations in the ratio of biogenic (Ca) to detrital (Ti) sediments are a reliable proxy for weight % CaCO3, with higher values during interglacial and interstadial stages and lower values occurring during glacial and stadial periods. On orbital scales, Ca/Ti minima mainly reflect dilution of biogenic carbonate by enhanced clay input in response to changing sea level (Thomson et al., 1999; Hodell et al., 2013b), while on millennial time scales, Ca/Ti minima reflect decreases in carbonate productivity (Hodell et al., 2013b) during cold events, and correspond to heavier planktonic $\delta^{18}O$ values and alkenone SST decreases. Correlation among coccolithophore variations and Ca/Ti profile have not been documented so far through the investigated interval and may represent a valuable tool for improving documentation of suborbital variability and chronology of the Site.

Coccolithophores represent a major component of marine phytoplankton and are sensitive indicators of variations in surface water properties such as temperature, productivity, salinity, and turbidity within the photic zone (McIntyre and Bè, 1967; Winter et al., 1994; Brand, 1994; Kleijne, 1990; Ziveri et al., 1995; Baumann et al., 2005). They benefit from oligotrophic conditions in warm and stratified waters from low and middle latitude regions (McIntyre and Bè, 1967; Honjo and Okada, 1974; Cortes et al., 2001) and also constitute an important contributor to the phytoplankton community in mature upwelled waters (Winter, 1985; Mitchell-Innes and Winter, 1987; Giraudeau, 1992; Ziveri et al., 1995). The investigated area is located at the

boundary between two coccolithophore biogeographic zones, the transitional and the subtropical zones (McIntyre and Bè, 1967). Abundance and distribution of coccolithophore in the area are related to the wind-driven upwelling productivity system (Moita, 1993; Abrantes and Moita, 1999; Silva et al, 2009). We present the first results on coccolithophore assemblage at Site U1385 which are interpreted in terms of past productivity and paleoclimate changes at glacial–interglacial and millennial time-scale. An additional indicator of primary paleoproductivity is also provided by total concentration of di and triunsaturated C_{37} alkenones. Finally, the overall proxies are compared with the available benthic and planktonic $\delta^{18}O$ records and Ca/Ti profile (Hodell et al., 2013a; Hodell et al., in this issue) and new benthic and planktonic $\delta^{13}C$ dataset.

2. Site location and modern oceanographic setting

Site U1385 was drilled using the advanced piston corer on the lower slope of the southwestern Iberian margin (37°34.285′ N, 10°7.562′W; 2578 m b.s.l.) (Fig. 1). Lithology mainly consists of nannofossil muds and nannofossil clays, with varying proportions of biogenic carbonate and terrigenous sediment (Expedition 339 Scientists, 2013). The average sedimentation rate is about 10 cm/kyr (Fig. 2a) according to Expedition 339 Scientists (2013). The modern hydrography at the western Iberian margin is influenced by the latitudinal displacement and seasonal intensification of Azores anticyclonic cell which, determining the intensity and changing direction of the offshore winds (e.g., Fiúza, 1984; Fiúza et al., 1998), are responsible for the seasonal upwelling. The main surface currents are traced in Fig. 1. The Portugal Current (PC, Fig. 1B) forms in the North-eastern Atlantic (McCartney and Talley, 1982) as a recirculation of the North Atlantic Current (NAC) and moves slowly southward along the Iberian margin from 45° to 30°N, centered west of 10°W in winter (Peliz et al., 2005). It includes a subsurface cold nutrient-rich and less salty water of subpolar origin (Eastern North Atlantic Central Water, $ENAC_{sp}$) forming during winter in the eastern North Atlantic (>45°N). The Azores Current (AzC, Fig. 1A, B) derives from the Gulf Stream and flows in large meanders eastward between 35° and 37°N through the mid-latitude North Atlantic. The northern boundary of the AzC forms the Subtropical Front (STF). The Iberian Poleward Current (IPC, Fig. 1B) originates from the AzC and includes a subsurface component (Eastern North Atlantic Central Water, $ENAC_{st}$) of less ventilated, nutrient-poor warm and saltier waters of subtropical origin (<45°N) (Frouin et al., 1990; Haynes and Barton, 1990), which moves quickly northward during winter (Peliz et al., 2005). The high seasonally-controlled temperature variability and zonal gradients are the main features of surface waters at the location of Site U1385 (Peliz et al., 2005; Eynaud et al., 2009). The northward displacement and strengthening of the Azores high-pressure cell causes upwelling-favorable northerly winds between April and October (Fiúza et al., 1982; Fiúza, 1984; Sousa and Bricaud, 1992; Sánchez and Relvas, 2003). The PC develops at this time and transports recently upwelled, cold and nutrient-rich waters along the Iberian margin (Wooster et al., 1976), stimulating the primary productivity.

In contrast, coastal convergence condition occurs during winter months when the Azores high strengthening decreases and moves southward. Surface circulation reverses and the northward transport, down to 1500 m depth (Relvas et al., 2007), of the warm nutrient-poor IPC (and $ENAC_{st}$), combined with the weaker northerlies and downwelling occurs (Peliz et al., 2005). Coccolithophores are the most tolerant group to these hydrological changes if compared with diatoms, that dominate during early spring to autumn upwelling events, and with dinoflagellates that benefit from maximum stratification during summer (Silva et al., 2009). In the area, with the exclusion of the periods of actual upwelling conditions, coccolithophores dominate the phytoplankton throughout the year, either during autumn and winter, when upwelling weakened and SST increases, and during short transition period from upwelling (summer) to downwelling (autumn) seasons (Abrantes and Moita, 1999; Silva et al., 2009; Moita et al., 2010).

With regard to deep waters, the saline, low nutrient- and oxygenated North Atlantic Deep Water (NADW) currently baths the site location. In the geological past, incursions of the deeper nutrient-rich, poorly ventilated and carbonate corrosive benthic $\delta^{13}C$-depleted Antarctic Bottom Water (AABW) are documented during glacials and short-term cooling stages of interglacials (Curry and Oppo, 2005; Martrat et al., 2007) when NADW production decreased or ceased.

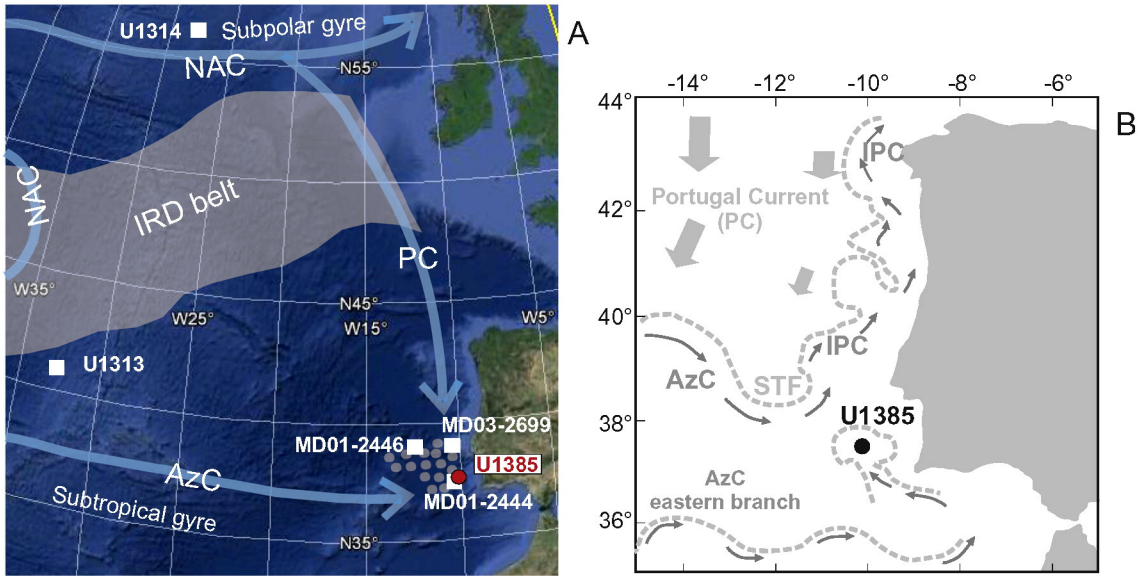

Fig. 1. (A) Location map of the studied Site U1385 and other sites mentioned in the text. (B) Surface water circulation during winter is redrawn from Voelker et al. (2010) according to Peliz et al. (2005). IPC = Iberian Poleward Current. STF = subtropical front. Ice-rafted detritus (IRD) belt is drawn according to Ruddiman (1977) for the last glacial period. Gray disks west of Iberian margin indicate signal of Heinrich type event during mid-Brunhes (see text for detail).

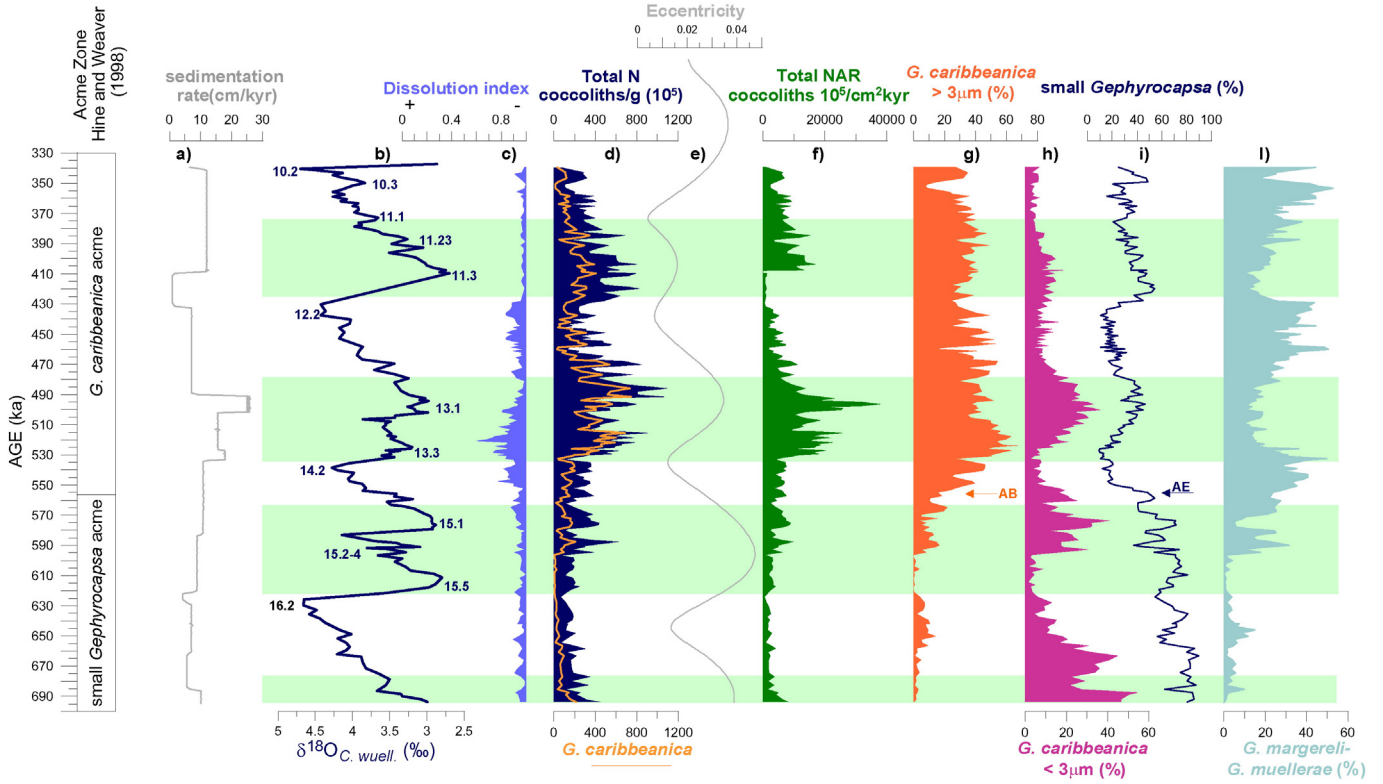

Fig. 2. (a) Sedimentation rate pattern from Hodell et al. (in this issue). (b) Benthic oxygen isotope record from Hodell et al. (2013a, in this issue). (c) Dissolution Index. (d) Total N of *G. caribbeanica* plotted on total N (total coccolith production). (e) Eccentricity according to Laskar et al. (2004). (f) Total coccolith accumulation rate (NAR). (g–l) Abundance patterns of selected coccolithophore taxa. Acme zones from Hine and Weaver (1998). AB: Acme beginning. AE: Acme end. Green bars indicate interglacial stages; substages are here indicated according to Bassinot et al. (1994).

3. Methods

3.1. Coccolithophores

Two hundred fifteen samples were analyzed from holes A, B, and D, between 47.19 and 81.71 crmcd (corrected revised meter composite depth). The adopted chronology follows the age model from Hodell et al. (this volume), which derives from correlation of benthic oxygen isotope record (Fig. 2b) to the reference stack of Lisiecki and Raymo (2005).

The investigated record corresponds to the interval MIS 16 to MIS 10 (693–339 ka). Samples were taken with a variable spacing ranging between 1–30 cm depending upon the sedimentation rate (Fig. 2a), providing a temporal resolution of about 1–2 kyr. A lower temporal resolution of ~3 kyr resulted in the lower portion of the record from about 590 ka down to the bottom of site. The adopted time resolution is adequate to appraise climate variability at glacial-to-interglacial and millennial time scale, including abrupt changes in sea surface water (e.g. H-type events) lasting about 2.4 kyr to 4.5/7 kyr during MIS 15-9 in the mid-latitude North Atlantic (Rodrigues et al., 2011).

Slides for coccolithophore analysis were prepared according to the method of Flores and Sierro (1997), to estimate absolute coccolith abundances. Quantitative analyses were performed using a polarized light microscope at 1000× magnification and abundances were determined by counting at least 500 coccoliths of all sizes. A variable number of visual fields were scanned for this counting, ranging from 4–5 in samples from interglacial periods and between 10 and 20, rarely up to 30, in glacial intervals. Reworked calcareous nannofossils were estimated separately during this counting. Additional area of slides was analyzed up to total 30 fields of view (about 1 mm^2) to improve the counting of taxa that resulted uncommon and rare in the 500-count. This supplementary counting was necessary due to the dominance of gephyrocapsids, which prevents the recognition of rare but environmentally important taxa. Percentage abundances are calculated on the total number of coccoliths per field of view, which may range between about 30 to 100 specimens, depending on the time interval. About 40 taxa were identified at species and subspecies level.

Variations in the assemblage were estimated using percentages, number of coccoliths/g of sediment (N) and Nannofossil Accumulation Rates (NAR), the last being calculated according to Mayer et al. (1992) and Flores and Sierro (1997). NAR values (coccoliths$*$cm$^{-2}*$kyr^{-1}) were estimated using the available wet bulk density (shipboard natural gamma ray density data) and derives from N$*$w$*$S, where N = coccolith/g of sediment; w = wet bulk density (g/cm^3); S = sedimentation rate (cm/kyr). In the absence of dry bulk density, wet bulk density is regularly used to estimate coccolithophore production (i.e. Grelaud et al., 2009; Stolz and Baumann, 2010; Marino et al., 2014). NAR is considered a proxy of paleoproductivity (Steinmetz, 1994; Baumann et al., 2004) although it may depend on dilution process due to changeable sedimentation rates and amount of terrigenous input, and on dissolution. For this reason we estimated the coccolith dissolution (DI) using the method of Dittert et al. (1999) modified by Amore et al. (2012) according to the following ratio: DI = small *Gephyrocapsa*/(small *Gephyrocapsa* + *Calcidiscus leptoporus*). High values of DI indicate good preservation.

With regard to the taxonomy of gephyrocapsids, which are a major component of the assemblage, we followed the criteria adopted in Maiorano et al. (2013), while the adopted coccolithophore proxies of surface water conditions are reported in the Appendix A.

3.2. C_{37} alkenones and stable carbon isotope

Alkenones are constituents of the autochthonous biomass synthesized by the coccolitophore flora which provide one of the geochemical tools most widely used to reconstruct past SST. We present total alkenone of 37 carbon atoms concentration interpreted as an indicator of phytoplankton productivity. Total alkenone concentration has been quantified from the total lipid extraction (TLE) of 505 samples from holes D and E. After freeze drying the samples were prepared following the procedure outlined in Villanueva et al. (1997). The organic compounds were extracted by sonication using dichloromethane and the extracts hydrolyzed with 6% potassium hydroxide in methanol to eliminate interferences from wax esters. The neutral lipids were then extracted with hexane, evaporated to dryness under a N_2 stream and finally, derivatised with bis(trimethylsilyl)trifluoroacetamide. The TLE fraction were analyzed in the DivGM's Varian Gas chromatograph Model 3800 equipped with a septum programmable injector and a flame ionization detector (Rodrigues et al., 2011) and some samples were analyzed by Bruker GC–MS in order to identify the mass spectrum of each compound. Sample resolution for this dataset varies between 0.1–1 kyr and rarely between 1–5 kyr. During MIS 15.2–4 (582–592 ka) a lower resolution dataset is currently available.

With regard to planktonic (*Globigerina bulloides*) and benthic (*Cibicidoides wuellerstorfi*) carbon isotope analysis the method is the same as that described by Hodell et al. (in this issue) for oxygen isotopes. Sample resolution varies between 0.7 and 4 kyr; lower resolution is available at MIS12/11 transition where a gap in the dataset, lasting about 20 kyr, currently occurs.

4. Results

Coccolithophore assemblages are generally well preserved with dissolution index showing high values through the record, ranging between 1 and 0.9 (Fig. 2c) which means that dissolution has not altered significantly the assemblage. Minima values are recorded through the MIS 14/13 transition and at restricted intervals within MIS 12, indicating slightly higher dissolution phases.

The total N varies between 57×10^5 and 1098×10^5 coccoliths/g sediment (Fig. 2d) and shows a stepwise increase through the record. Low coccolith concentrations occur in the sediment from MIS 16 to the lowermost part of MIS 15, when the small gephyrocapsid group dominates on the entire assemblage (Fig. 2i). From 595 ka, total N starts to increase concomitant to the rise of *Gephyrocapsa caribbeanica* > 3 μm and to the reduction of small *Gephyrocapsa* (Fig. 2g, i), while a more prominent rise in abundance marks the beginning of MIS 13 at 529 ka (Fig. 2d). Throughout the record, the total N increases during interglacials and particularly during MIS 13 and 11, with maximum values during MIS 13. A weak increase is also observed during MIS 14, and several abrupt shorter-term variations are recorded (Fig. 2d). The total NAR varies from 507×10^5 to 37666×10^5 coccoliths/cm^{2}kyr (Fig. 2f). The general trend follows the total N, although a distinct NAR decrease characterizes the lowermost part of MIS 11. Among the glacials the lowest NAR values are recorded within MIS 16 and 12.

G. caribbeanica and small *Gephyrocapsa* (with open central area) are the dominant taxa through the record (Fig. 2g–i). Small *Gephyrocapsa* prevails in the lower part of the record from MIS 16 up to MIS 15 reaching percentage even higher than 80%, whereas *G. caribbeanica* (>3 μm) gradually increases from MIS 15 (595 ka) and dominates from MIS 14 (555 ka) onwards. This abundance reversal of the genus *Gephyrocapsa* documents the boundary between the world-wide Acme Zones of the Middle Pleistocene (Hine and Weaver, 1998) and specifically between the small *Gephyrocapsa* and the *G. caribbeanica* Acme Zone (Fig. 2). *Gephyrocapsa margereli–G. muellerae* (>3 μm) group is also an important component of the assemblage from MIS 15.2-4 (Fig. 2l), displaying higher abundances, up to 40%, during glacial stages. The warm water taxa (wwt) group shows significant fluctuations (Fig. 3c), with higher values during interglacials and maximum during MIS 15 (up to 4%) when also high variability is recorded.

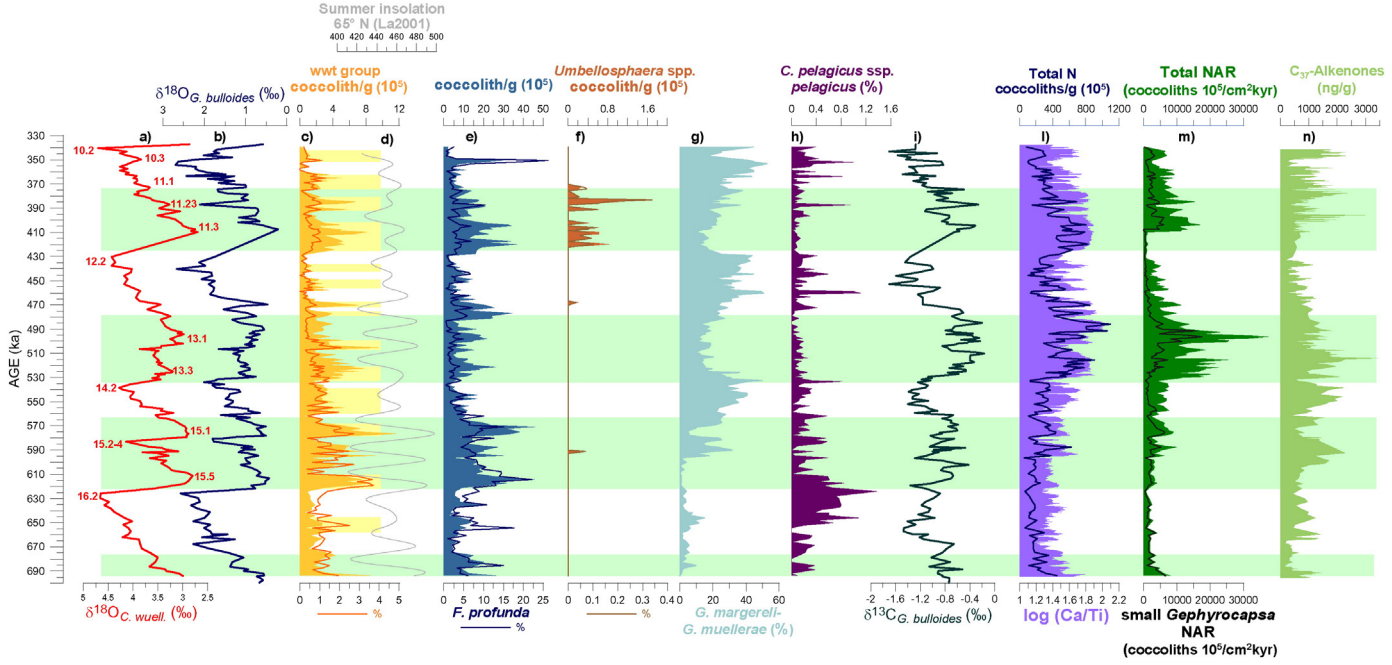

Fig. 3. (a, b) Benthic and planktonic oxygen isotope records from Hodell et al. (2013a, in this issue). (c) Abundance patterns of warm water taxa (wwt). (d) Summer Insolation according to Laskar et al. (2004). (e–h) Abundance patterns of selected coccolithophore taxa. (i) Planktonic carbon isotope record. (l) Total coccolith production (Total N) plotted against Ca/Ti ratio (Hodell et al., 2013a). (m) Total NAR of small *Gephyrocapsa* plotted on pattern of total NAR. (n) Pattern of C_{37}-Alkenones. Green bars indicate interglacial stages; substages are here indicated according to Bassinot et al. (1994). Yellow bars indicate surface water warming phases based on increase of warm water taxa (wwt). (For interpretation of the references to color in this figure legend, the reader is referred to the web version of this article.)

Specifically, the wwt group clearly increases at 621 ka, at the onset of MIS 15 (Fig. 3c) and displays enhanced abundances within MIS 15.5 and 15.1 in agreement with the $\delta^{18}O_{G.bulloides}$ profile (Fig. 3b). Slight increases are also coeval with MIS 13.3 and 13.1 and within MIS 11.3 and 11.23. Among the glacials, MIS 14 records the highest abundances of the wwt group, while lowest values occur during MIS 12. Shorter-term increases of the wwt group, lasting about 4–10 kyr, characterize glacials MIS 12 and MIS 10 (Fig. 3c). *Florisphaera profunda* is present throughout the record with abundances ranging between 2 and 15% and sharp peaks occasionally reaching values higher than 20% (Fig. 3e). The percentage pattern of this taxon shows a decreasing trend from MIS 14-13 upwards. The lowest values of the taxon are recorded throughout MIS 13, if compared with the younger and older interglacials. Subordinate taxa are also represented by *C. leptoporus* s.l. (*C. leptoporus* small 3–5 μm, *C. leptoporus* intermediate 5–8 μm and *C. quadriperforatus* 8–10 μm), *Coccolithus pelagicus* s.l (*C. pelagicus* ssp. *pelagicus* 6–10 μm, *C. pelagicus* ssp. *braarudii* 10–13 μm and *C. pelagicus azorinus* 14–16 μm), *Syracosphaera* spp. (mainly *S. histrica* and *S. pulchra*), *Helicosphaera* spp. (not shown here), *Umbellosphaera* spp.. The latter, although very rare in the assemblage, has a limited range within MIS 11 (Fig. 3f). Among subordinate taxa, *C. pelagicus* ssp. *pelagicus* displays a long-term increase within MIS 16, while 14 prominent short terms peaks of the taxon occur through the record (Fig. 4e). They are in phase with decreases of total N (Fig. 4d) and occasionally with peaks of *G. margereli–G. muellerae* > 4 μm (Fig. 4f). Rarely a concomitant *Helicosphaera carteri* and *F. profunda* increase is also observed (Fig. 4h–i). Reworked calcareous nannofossil specimens are generally lower than 2%, except in an interval during MIS 16, with abundance peaks as high as 6% (Fig. 4g). Distinctive short-term peaks, up to 4% in abundance, are coeval with spikes of *C. pelagicus* ssp. *pelagicus* (Fig. 4e, g).

Through the investigated interval the total C_{37} alkenone concentration (Fig. 3n) varies between 102.76 ng/g and a maximum of 3429.76 ng/g. The lowest values are recorded during MIS 16, MIS 15.1 and 15.5, MIS 12 and in the beginning of MIS 11. Alkenone concentration increases within MIS 15.2-4, MIS 14, MIS 13.3 where maxima values are recorded, in the MIS 11 glacial inception and MIS 10.

5. Discussion

5.1. Long-term cycle in coccolithophore production

The distinct increase observed in N and NAR at MIS14/13 transition, starting at 530 ka, with *G. caribbeanica* becoming the most important taxon in terms of coccolith production (Fig. 2d), provides evidence of the beginning of the wide-scale MB blooming of *G. caribbeanica* (Bollmann et al., 1998; Baumann and Freitag, 2004). Prominent N and NAR increases at the studied site occur during interglacial MIS 13 and MIS 11. Although the whole stratigraphic range of the MB blooming of *G. caribbeanica* is not recovered, the observed increase in coccolithophore production is part of a long-term eccentricity driven cycle during a 400 kyr eccentricity minimum (Fig. 2d–e). This datum is consistent with the hypothesis of a relation between phytoplankton growth rate, and therefore coccolithophore production, with the 400 kyr eccentricity forcing (Rickaby et al., 2007). In fact, blooms of coccolithophore show day length preferences (Balch, 2004) and they are supposed to occur optimally when maximal season length is coupled with the maximal solar insolation, that is, when eccentricity is at a minimum (Rickaby et al., 2007).

The slight dissolution increase coinciding with MIS 14 and 13 transition (Fig. 2c), which is concomitant with the gradual increase of *G. caribbeanica* > 3 μm (Fig. 2g), may reflect the onset of a period of global carbonate dissolution, the MB dissolution interval (Droxler et al., 1988; Barker et al., 2006). However, the high values of the dissolution index do not appear so relevant at the site location, which agrees with data from nearby record (core MD03-2699) for the same time interval (Amore et al., 2012).

The strong positive correlation observed between fluctuations of N and Ca/Ti content, especially from MIS 13 onwards (Fig. 3l), suggests that coccolith-derived carbonate is the dominant contributor to carbonate production in the studied interval and sustains the idea that the heavily calcified *G. caribbeanica* is the most important producer of carbonate through the MB interval (Bollmann et al., 1998; Flores et al., 1999; Baumann and Freitag, 2004; Baumann et al., 2004; Lopez-Otalvaro et al., 2008; Marino et al., 2014; Balestra et al., in this issue). These data support the use of coccolithophores as proxy of carbonate production through the studied interval. General trends in the total NAR (Fig. 3m) follow the pattern in the C_{37} alkenones (Fig. 3n), further supporting the interpretation of NAR as coccolithophore productivity pulses.

5.2. Coccolithophores and surface water conditions

5.2.1. Interglacial variability

The total N and NAR increase during interglacials (Fig. 3l–m), particularly during MIS 13 and MIS 11, is believed to reflect the response of coccolithophores to prevailing warmer, moderately productive surface water conditions and to the *G. caribbeanica* blooming starting at MIS 14/13 transition. A reduced productivity characterizes MIS 15, before the MB beginning, as highlighted by lower NAR. The productivity pattern deduced from coccolithophore proxies at glacial/interglacial scale is in good agreement with the $\delta^{13}C_{G.\ bulloides}$ profile (Fig. 3i) that suggests higher nutrient availability during interglacials and particularly during MIS 13, and with the overall pattern of C_{37} alkenones (Fig. 3n). This productivity pattern is consistent with an upwelling-related regime and in fact it appears well comparable with data from the similarly located core MD03-2699 (Rodrigues et al., 2011), while it differs from what recorded at the North Atlantic IODP Site U1313 (Stein et al., 2009), outside of the western Iberian upwelling, where productivity was higher during the glacials, reflecting an open ocean productivity regime. Enhanced abundances of the wwt group during MIS 15, 13 and 11 (Fig. 3c), is in agreement with a sea surface warming during these interglacials.

The enhanced abundances of the wwt group during MIS 15 (Fig. 3c) suggest that the influence of subtropical waters was strengthened during this interval, relative to the younger interglacials. The highest values of the wwt group observed from 621 to 611 ka indicate MIS 15.5 as the warmest phase. The high amplitude fluctuations of the wwt group appear well related to high seasonality characterizing this interglacial (eccentricity maximum and high precession/insolation amplitude) (Fig. 3d). The higher abundance of the deep dwelling *F. profunda* (Fig. 3e), which substantially varies as the wwt group, suggests reduced surface water productivity coupled with warmer temperatures down to thermocline depth, especially during MIS 15.5 and 15.1. The opposite pattern between C_{37} alkenones (Fig. 3n) and *F. profunda* in this interval is consistent with indication of lower surface water productivity during MIS 15.5 and 15.1. We propose that the coccolithophore behavior reflects an intensified contribution of the subtropical AzC during MIS 15.5 and 15.1 at the site location. Based on the modern hydrographic conditions this scenario could be related to a southward migration of the subtropical Azores High and weaker northerly winds, leading to a northward displacement of the warm AzC (Volkov and Fu, 2010; Peliz et al., 2005; Relvas et al., 2007; Sánchez et al., 2007). A different situation occurs during 15.4-2. In fact, several shifts in the abundance of the wwt group (Fig. 3c) point to less stable surface water conditions. *G. margereli–G. muellerae* 3–4 μm (Fig. 3g) as well as *C. pelagicus* ssp. *pelagicus* (Fig. 3h) show increase in their abundance in agreement with the occurrence of cold surface water advection at this time. In addition, the presence of productive surface waters can be also inferred, mainly from the increase in C_{37} alkenones, which is consistent with the intensification of northerly

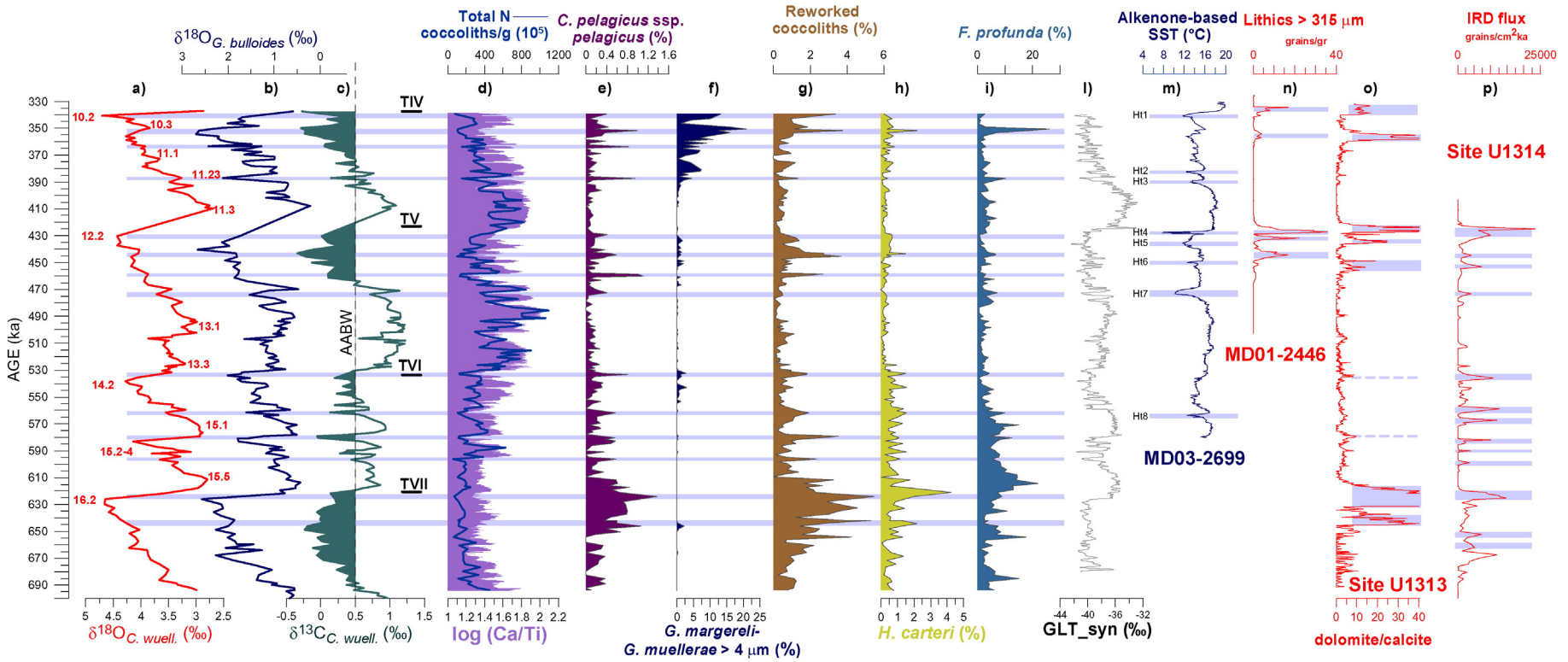

Fig. 4. (a, b) Benthic and planktonic oxygen isotope records from Hodell et al. (2013a, in this issue). (c) Benthic carbon isotope record; vertical line indicates typical values for AABW according to Adkins et al. (2005). (d) Total coccolith production (Total N) plotted against Ca/Ti ratio. (e–i) Patterns of selected coccolithophore data. (l) Synthetic reconstruction of Greenland temperature variability (GL_{T}_syn) from Barker et al. (2011). (m) Sea Surface Temperature (SST) and inferred Heinrich type events (Ht1–8) at Core MD03-2699 from Rodrigues et al. (2011). (n) Lithics concentration and inferred Heinrich-type events at Core MD01-2446 from Voelker et al. (2010). (o) Dolomite/calcite ratio as ice-rafted detritus indicator at Site U1313 from Stein et al. (2009) and Naafs et al. (2011). (p) IRD flux at Site U1314 from Alonso-Garcia et al. (2011).

winds and southward advection of cold and nutrient-rich surface waters (Fiúza et al., 1982; Relvas et al., 2007).

During MIS 13, the high values of total NAR are correlated with persistent higher C_{37} alkenone concentration (Fig. 3n). However, it is noteworthy that the sharp peak of NAR during MIS 13.1 could be overestimated due to strong variation in sedimentation rate (Fig. 2a). During MIS 13, the trend in the total NAR is obviously related to the onset of the *G. caribbeanica* acme (Fig. 2g). However, a distinctive increase is also recorded in the NAR of small *Gephyrocapsa* (Fig. 3m), taxa related to eutrophic conditions and upwelling in surface waters (Gartner et al., 1987; Gartner, 1988; Okada and Wells, 1997; Takahashi and Okada, 2000; Colmenero-Hidalgo et al., 2004; Flores et al., 2005; Amore et al., 2012). This suggests that the total NAR increase is not only related to the phylogenetic adaptation and dominance of *G. caribbeanica* (Bollmann et al., 1998), but also reflects environmental conditions. In addition, the low abundances of *F. profunda* throughout MIS 13 sustain the occurrence of unstable and mixed surface waters. Enhanced total NAR values are concomitant with MIS 13.3 and MIS 13.1, and are in agreement with higher $\delta^{13}C_{G.\ bulloides}$ record (Fig. 3i). In these intervals the proliferation of coccolithophores may reflect more intense upwelling conditions and can be a response to favorable conditions related to mature upwelled waters occurring during summer–autumn seasons (Silva et al., 2008, 2009). More intense prevailing upwelling characterized the MIS 13.1 as deduced by peaks of total NAR, concurrent with distinct increases in NAR of small *Gephyrocapsa* (Fig. 3m). Similarly to the present day behavior of small taxa such as *Emiliania huxleyi* (Silva et al, 2008, 2009), small *Gephyrocapsa* may have benefit from favorable conditions at the beginning of the spring–summer upwelling. At this level, differently than it would be expected, the wwt group curve does not display a concomitant increase (Fig. 3c), likely because of higher nutrient availability and unstable surface waters that resulted in unfavorable conditions for warm and oligotrophic taxa, similar to the results of Marino et al. (2014) at core MD01-2446. The coccolithophore trend during MIS 13 supports previous findings from Iberian margin, suggesting more variable and productive surface waters during this interval (Voelker et al., 2010; Rodrigues et al., 2011) and may also be in relation with a major reorganization of the global ocean carbon reservoir as deduced from global maximum in $\delta^{13}C$ (Hodell et al., 2003; Wang et al., 2003; Barker et al., 2006), which records maxima values also at the studied site (Fig. 3i). Notably, at this time a switch in the percentage abundance of *F. profunda* (decreasing trend, Fig. 3e) and of *G. caribbeanica* > 3 μm (increasing trend, Fig. 2g) may be observed, supporting a linkage between surface ocean structure and the "$\delta^{13}C_{max}$ II" event (Wang et al., 2003).

At MIS12/11 transition, despite the lower resolution in $\delta^{18}O$, the increase in the wwt group recorded at about 425 ka (Fig. 3c), as well as concomitant total N increases (Fig. 3l), mark ameliorated climate conditions, following MIS 12 deglaciation, clearly tracing the onset of MIS 11. Evidence of surface water warming coincides with the first peak of the weak summer insolation maximum at the base of MIS 11 (Fig. 3c–d) and it is in good agreement with the age of SST increase recorded at the Iberian margin at core MD03-2699 (426.6 ka, Rodrigues et al., 2011), with the wwt group increasing at core MD01-2446 (426 ka, Marino et al., 2014), and with several other North Atlantic and continental records (e.g. Oppo et al., 1998; Desprat et al., 2005; de Abreu et al., 2005; Stein et al., 2009; Kandiano et al., 2012). During MIS 11.3 the wwt group depicts a long lasting surface water warming if compared to the other warm phases of previous interglacials. Considering the pattern observed within MIS 15, it might be related to the weaker insolation forcing characterizing MIS 11 (Fig. 3d), further implying that coccolithophore variations in the area are affected by seasonality. During MIS 11.3, despite the increase of total N (Fig. 3l), the singular total NAR pattern, characterized by the lowest abundances through 425–409 ka (Fig. 3m), suggests that surface water productivity was dramatically reduced. It is noteworthy that in this interval total NAR values are strongly affected by very low sedimentation rate (Fig. 2a), indicating a condensed section or a brief hiatus (Hodell et al., in this issue). On the other hand the concurrent low values of C_{37} alkenones (Fig. 3n) support the occurrence of low productive surface water conditions, while the low resolution in the $\delta^{13}C$ dataset (Fig. 3i) does not provide valuable information in this interval. Based on the present results, this data-pattern may reflect the response of the coccolithophore assemblage to intense stratification within the photic zone. Many coccolithophore taxa are k-selected and therefore their total abundance and diversity are known to increase during stable, stratified and oligotrophic conditions (Baumann et al., 2005); on the other hand few coccolithophore species are adapted to eutrophic environment where high coccolith accumulation rates occur (Baumann et al., 2004). Surface water stratification and low nutrient availability in surface water is also supported by concomitant increases in abundance of the deep-dwelling *F. profunda* (Fig. 3e). Additional evidence is provided by the sudden appearance in the assemblage of *Umbellosphaera* spp. at 420 ka (Fig. 3f), which may reflect a new available habitat in stratified waters and well-developed oligotrophic conditions down to the middle of the photic zone. Such a surface water condition could result from continuous and enhanced influence of the subtropical waters at the site during this interval, in agreement with mid-latitude North Atlantic records (de Abreu et al., 2005; Martrat et al., 2007; Helmke et al., 2008; Hagino and Kulhanek, 2009; Stein et al., 2009; Voelker et al., 2010; Rodrigues et al., 2011; Kandiano et al., 2012; Marino et al., 2014). However, we cannot exclude that decreased detrital input from land, resulting from the high sea level stand during MIS 11.3 (Bintanja and van de Wal, 2008), may have also induced both enhanced oligotrophic conditions and minor coccolith dilution (high total N), due to reduced delivery of land-derived nutrients and decreased detrital input, respectively. High values in the Ca/Ti profile may be also consistent with a low dilution effect. Reduced continental input at the beginning of MIS 11 at Site U1385 is also sustained by the pattern observed in the terrigenous biomarker (Rodrigues et al., 2014). At the end of MIS 11.3, starting from 409 ka, the recovery of coccolithophore productivity is likely related to reduced influence of subtropical advection and/or sea level lowering, even though C_{37} alkenone concentration records a slightly late increase. The decreasing of total NAR upwards, follows the cooling trend toward the MIS 10 glacial inception.

5.2.2. Glacial variability

Among the glacials, the lower N and NAR values (Fig. 3l–m), as well as low abundances of the wwt group, particularly during MIS 16, MIS 12 and the upper MIS 10 (Fig. 3c), suggest unfavorable conditions for coccolithophore growth, likely related to severe climate conditions occurring during these intervals, due to large northern Hemisphere ice sheet expansion as revealed by the highest $\delta^{18}O$ values. The increase in abundance of *C. pelagicus* ssp. *pelagicus*, mainly during MIS 16, and of *G. margereli–G. muellerae* during MIS 14, 12 and 10, sustain the dominance of cold surface water conditions during these intervals.

The long lasting increase in abundance of *C. pelagicus* ssp. *pelagicus* between 647 and 624 ka, in the late MIS 16 (Fig. 3h), suggests a more persistent influence of subpolar waters at the site location, in agreement with the distribution of *C. pelagicus* ssp. *pelagicus* at the northernmost Atlantic Site ODP 980 (Marino et al., 2011). This observation is consistent with North Atlantic data (Wright and Flower, 2002), meaning a southward position of the Artic Front during the glacials preceding the end of the MPT (MIS 16) and sustaining the world-wide indication that MIS 16 was a long lasting and severe glacial stage (Lisiecki and Raymo, 2005; Tzedakis et al., 2006; Bintanja and van de Wal, 2008; Hodell et al, 2008). During MIS 14, the pattern of the wwt group (Fig. 3c), supports the influence of subtropical waters on the Iberian margin during this stage (Voelker et al., 2010) and agrees with results deriving from several records indicating MIS 14 as a weak glacial (e.g. Mix et al., 1995; Wright and Flower, 2002; Billups et al., 2006; Hodell et al., 2008; Lang and Wolff, 2011; Rodrigues et al., 2011). Total NAR values during MIS 14 are also slightly higher if compared with older

and younger glacials (Fig. 3m) and are comparable with the C_{37} alkenone increase (Fig. 3n), supporting the occurrence of a different circulation pattern during this interval over the Iberian margin (Voelker et al., 2009; Rodrigues et al., 2011).

The lowest NAR values occurring during MIS 12.2 (Fig. 3m), combined with decreases in total N (Fig. 3l), suggest the development of severe cold conditions at the glacial maximum in agreement with the heavy benthic $\delta^{18}O$ values, close to TV (Fig. 3a). This is also supported by the increase of *G. margereli–G. muellerae* (3–4 μm) and *C. pelagicus* ssp. *pelagicus* (Fig. 3g–h) and the concomitant lowest abundance of the wwt group (Fig. 3c). Unfavorable conditions to coccolithophore growth can be linked to concomitant increases in IRD (see next section) at this time. A possible dissolution effect should be also considered, based on the DI pattern (Fig. 2c). In addition, higher frequency variability in surface water conditions during glacials MIS 12 and 10 is testified by shorter-term increases of the wwt group (Fig. 3c). This is also supported by depleted values of $\delta^{18}O_{G.\ bulloides}$ (Fig. 3b), although low resolution is currently available in the latter dataset, particularly during MIS 12. Concurrent increases in total N, NAR, C_{37} alkenone and carbonate content (Fig. 3l–n) are evidences of relative increased productivity during these interstadials. The latter are interrupted by short pulses of *C. pelagicus* ssp. *pelagicus* implying short-term advection of subpolar waters coupled with reduced productivity as suggested by lower values of N, NAR and C_{37} alkenones (Fig. 3l–n).

5.3. Millennial-scale coccolithophore assemblage variations

The present coccolithophore data-set from Site U1385 provides evidences of abrupt and short-term climate variability through the studied interval (Fig. 4). Specifically, *C. pelagicus* ssp. *pelagicus* and *G. margereli–G. muellerae* > 4 μm patterns (Fig. 4e–f) highlight the occurrence of surface water cooling as well as a decrease in coccolithophore production, likely related to the arrival of subpolar cool and low saline waters at the core location, and southward migration of Polar Front, which may have developed unfavorable surface water conditions for coccolithophore growth (Stein et al., 2009; Stolz and Baumann, 2010; Marino et al., 2014). Although data on IRD fluxes are lacking in our dataset, we tentatively correlate the pattern of *C. pelagicus* ssp. *pelagicus* (Fig. 4e) and of concomitant enhanced reworking (Fig. 4g) to increases in iceberg-derived detritus, in agreement with recent coccolithophore data from the Iberian margin (Amore et al., 2012; Marino et al., 2014). However, the influence of detrital input from the Iberian peninsula during significant low sea level stands may not be excluded. The coeval increase of *F. profunda* (Fig. 4i), although sporadic, may be a response to stratified, turbid and fresher surface waters related to iceberg discharge and warmer subsurface water at the thermocline/nutricline, that favored the deep dwelling taxon. In previous literature *F. profunda* has been recorded in the Gulf of Cadiz during HE of the last glacial (Colmenero-Hidalgo et al., 2004) and on the Iberian margin during stadials of the last 70 kyr attesting the arrival of Arctic surface waters (Incarbona et al., 2010). However, from the present record the response of this taxon is somewhat ambiguous to the H-type events of the MB interval as also observed in core MD01-2446 (Marino et al., 2014).

The short-term variations based on the coccolithophore assemblage agree with the prominent abrupt minima recorded in the Ca/Ti profile (Fig. 4d), supporting the definition of rapid shifts in the coccolithophore assemblage as prominent cooling events. In fact, in this area, Ca/Ti minima on millennial time scale, correspond to severe cold events, reflecting decreases in carbonate productivity (Hodell et al., 2013a,b), although a relation with increased detrital sedimentation has also been indicated in the deep Portuguese margin (Lebreiro et al., 2009). Evidences of surface water-cooling are also well recorded in almost all of the events by coeval heavier values of $\delta^{18}O_{G.\ bulloides}$ (Fig. 4b). Some of the events are also concomitant with depleted benthic $\delta^{13}C$ values (Fig. 4c) likely in response to poor deep water ventilation related to changes in the AMOC strength due to iceberg discharge and enhanced meltwater flux (Broecker et al., 1992; Maslin et al., 1995; Zahn et al., 1997; Schönfeld et al., 2003; McManus et al., 2004). However, higher resolution of oxygen isotope data set might improve this correlation.

The temporal distribution of the abrupt events at Site U1385 suggests that short-term pulses of subpolar water affected the Iberian margin not only during the glacials MIS 16, 12 and 10 but even during MIS 15 and at the end of MIS 11 (Fig. 4), highlighting intra–interglacials variability.

During MIS 16 the most prominent peaks of *C. pelagicus* ssp. *pelagicus* and reworked calcareous nannofossil taxa (Fig. 4e, g) are recorded at 646 ka and 624 ka concurrent with low total N (Fig. 4d). This could be related to processes of major IRD discharge occurring during the latest part of MIS 16 and at TVII. This is also supported by distinct abrupt increases in the abundance of *H. carteri* (Fig. 4h) particularly at TVII, when the species has its maximum abundance in the studied record. Peaks of this taxon, related to fresher and more turbid upper layer, have been documented at terminations for MIS 1 to 14 in the Southern Ocean (Flores et al., 2003) and during HE (Colmenero-Hidalgo et al., 2004) in the Gulf of Cadiz. Coeval HE/detrital layers were identified during MIS 16 at Site U1308 and Site U1302-03 from Hodell et al. (2008) and Channell et al. (2012) respectively (detrital layers 16.1 and 16.2 in Channell et al., 2012). Prominent IRD peaks have been also recorded at Site U1313 (Fig. 4o) (Stein et al., 2009; Naafs et al., 2011). High abundances of IRD are also manifest at the ODP Site 980 during MIS 16 (Wright and Flower, 2002) and a prominent IRD peak marks TVII at the western Northern Atlantic Site U1314 (Fig. 4p), which highlights a main source area from Greenland and Iceland (Alonso-Garcia et al., 2011). Two abrupt cold events are detected within MIS 15.2-4 (at 596 ka and 580 ka) (Fig. 4). They are identified on the basis of abundance peaks of *C. pelagicus* ssp. *pelagicus* associated with low total N and NAR and peaks of reworking. High resolution data are not available from the Iberian margin in this interval, because the recent studies have mainly focused on climate variability during younger intervals (Martrat et al., 2007; Stein et al., 2009; Voelker et al., 2010; Rodrigues et al., 2011; Amore et al., 2012). However, the occurrence of abrupt cooling at Site U1385 is in agreement with sharp and prominent negative shifts in the pattern of the synthetic reconstruction of Greenland temperature variability (GL_T_syn) from Barker et al. (2011) (Fig. 4l). High millennial-scale climate variability during MIS 15.2-4 is also proved by multiple short-term fluctuations in the wwt group pattern (Fig. 3c). The coccolihophore data set seems consistent with the hypothesis that cold events recorded during MIS 15.2-4 are related to Greenland climate instability suggesting that the advection of subpolar waters may have affected the Iberian margin at this time. The event at 580 ka is also concurrent with a sharp decrease in benthic $\delta^{13}C$ values, below 0.5‰ (Fig. 4c), that may imply the entrance of the southern bottom water source (AABW) during this short cold episode of the interglacial. Two detrital layers have been also identified at Site U1302/03 during MIS 15 (Channell et al., 2012). Data available from the North Atlantic Site U1313 indicate the occurrence of two minor "Heinrich-like" events during MIS 15.2 (Stein et al., 2009) (Fig. 4o). Based on their mineralogical signature, Stein et al. (2009) assumed a source from Greenland, Labrador or Scandinavia rather than Hudson Bay. However, the authors did not identify these events with certainty as IRD events because the occurrence of tephra grains could also indicate the Azores Island volcanoes as possible source area. Moreover ice-rafting events were observed in MIS 15.2 at Site U1314 and during strong oscillations in the benthic $\delta^{13}C$, indicating a reduction in the deep water convection in the Norwegian Greenland Sea and in the generation of Iceland Scotland Overflow water (Alonso-Garcia et al., 2011). IRD peaks during MIS 15.2/15.1 transition have been recorded as well at Site 980 (Wright and Flower, 2002) which is ideally located to record ice rafting from both Hudson Bay and Scandinavian and Greenland sources.

From MIS 15/14 transition up to MIS 10 the coccolithophore proxies for abrupt subpolar water advection at the core location are well correlated to the SST decreases recorded in the Iberian margin at the northern

Core MD03-2699 (Ht1–Ht8, Rodrigues et al., 2011) (Fig. 4m) and/or at the Core MD01-2446 (Fig. 4n), based on increases in lithic concentration (Voelker et al., 2010) and patterns of selected coccolithophores (*C. pelagicus* ssp. *pelagicus*, reworked calcareous nannofossils, *G. margereli–G. muellerae* > 4 μm), and *N. pachyderma* left as well (Marino et al., 2014). An additional event in our record occurred at TVI (533 ka). At this level, the peaks of *C. pelagicus* ssp. *pelagicus* and reworked calcareous nannofossils (Fig. 4e, g) correlate with a synchronous IRD peaks at Site U1314 (Fig. 4p) and, despite its minor intensity, also at Site U1313 (Fig. 4o). A coeval detrital layer (numbered as 13.6) is recorded at Site U1302/03 (Channell et al., 2012). Within MIS 10, the cold event at 363 ka does not appear to have an equivalent in other records both on the Iberian margin and North Atlantic record (Fig. 4m–p). In the upper part of MIS 10 the abrupt cooling events (at 351 ka and 340 ka) marked by peaks of *C. pelagicus* ssp. *pelagicus*, as in the older intervals, and by concomitant and prominent increases of *G. margereli–G. muellerae* > 4 μm (Fig. 4f) support southward influx of polar-subpolar waters (Girone et al., 2013; Marino et al., 2014). The abrupt cooling at 351 ka at Site U1385 is well correlated with the signal of IRD flux at Core MD01-2446 (Voelker et al., 2010) and Site U1313 (Stein et al., 2009; Naafs et al., 2011, 2013), whereas it was not recorded at Core MD03-2699. At this level a significant peak of *F. profunda* occurs (Fig. 4i), together with high abundance of reworked calcareous nannofossils and *G. margereli–G. muellerae* > 4 μm. The same pattern of *F. profunda*, suggesting water stratification and inverse thermocline condition, has been recorded concomitant to the IRD flux at 356 ka at the northwestern Core MD01-2446 (Fig. 4n) implying that these oceanographic conditions characterize this event on the Iberian margin.

Throughout the studied record a good comparison is seen between the short-lived climate coolings at Site U1385 and analogous ones in North Atlantic cores. Slightly different occurrence/non occurrence and chronology of Ht events among the sites have been noted. Ocean circulation, iceberg route path, source area and chronology of IRD may be possible causes of the observed differences (Hemming, 2004). In fact, as discussed above, Site U1313 mainly records IRD from Laurentide Ice-Sheet (Stein et al., 2009; Naafs et al., 2011, 2013), whereas an influence of ice-rafting from Greenland and European ice-sheets has been suggested at the cores MD03-2699 (Rodrigues et al., 2011) and MD01-2446 (Voelker et al., 2010; Marino et al., 2014) similar to Site U1314 (Alonso-Garcia et al., 2011; Naafs et al, 2013). The present data set will need supplementary proxies such as the IRD and *N. pachyderma* left records, SST data as well as higher resolution planktonic $\delta^{18}O$, in order to support the cooling events pointed out by coccolithophore assemblages, and their relationship with H-type events and front dynamics.

6. Conclusion

The coccolithophore signature at Site U1385 through MIS 16-10 points to varying surface water conditions, reflecting orbital and millennial scale climate variability. These are the result of the interaction among long-term modifications in the coccolithophore assemblage typical of the MB interval, wind-driven hydrographic changes and short-term Northern Hemisphere ice-sheet variability. With the present study, the high-resolution coccolithophore dataset at the Iberian margin, well known through MIS 13-9, is extended down to MIS 16. Differently from what recorded in mid-latitude open ocean records, a general trend of increased productivity is observed during interglacials, particularly during MIS 13 and the upper part of MIS 11, in response to the predominance of warm climate conditions and seasonal upwelling. Interglacial phases are marked by the increase of the wwt group whose pattern is consistent with previous data acquired on the Iberian margin through MIS 13-9. Warmer thermocline waters and reduced productivity during MIS 15.5 and 15.1 suggest a prominent influence of relative warm, nutrient-poor and less ventilated subtropical waters advected with the Azores Current. A southward migration of the subtropical Azores High and weaker northerly winds can be inferred during these times. Colder and more productive surface waters characterizes MIS 15.4-2, implying a southward advection of cold and nutrient-rich surface waters, likely in relation to intensified northerly winds. Highest productivity during MIS 13 is triggered by the worldwide-scale MB blooming of *G. caribbeanica* as well as by intensified upwelling events. During MIS 11.3, a long lasting warm surface water phase, during a period of low insolation forcing, is coupled with intense stratification and significantly reduced productivity within the photic zone. This pattern likely reflects continuous and enhanced subtropical water advection. Reduced delivery of land-derived nutrients during high sea level stand could have also been responsible for the significantly reduction of surface water productivity. The pattern of wwt group, here evaluated through a more extended time frame, highlights that surface water variability during interglacials reflects seasonality, with intense fluctuations occurring during periods of maximum insolation forcing. Glacial conditions through the investigated record are traced by the increase of *C. pelagicus* ssp. *pelagicus* and *G. margereli–G. muellerae*. A more persistent influence of subpolar waters and a southward position of the Polar Front can be inferred during MIS 16, based on a long-term increase of the subpolar *C. pelagicus* ssp. *pelagicus*. Weak glacial conditions developed during MIS 14, as deduced from the abundance of the wwt group, in agreement with previous findings. Superimposed on the orbital variability, coccolithophore records millennial scale modifications. Our reconstruction provides identification of 14 stadial-type episodes which are characterized by abrupt and short-term increases of the subpolar species *C. pelagicus* spp. *pelagicus* and/or of *G. margereli G. muellerae* > 4 μm, reworked taxa and decreased coccolithophore productivity. This pattern reflects brief advection of subpolar waters at the core location, which developed unfavorable surface water conditions for coccolithophore growth. The events are well comparable with heavy planktonic $\delta^{18}O$ values and, interestingly, also with Ca/Ti minima which may improve suborbital tuning of the site. Some of the events are also concomitant with depleted benthic $\delta^{13}C$ values, likely in response to the entrance of AABW. This evidence strengthens the connection between mid-latitude abrupt climate changes and high frequency variability in northern and southern polar regions down to MIS 16. Evidences for rapid coolings within interglacial MIS 15, which are recorded for the first time on the Iberian margin, sustain the occurrence of intra-interglacial instability likely linked to Greenland climate instability and temporary reduction in the AMOC. Most of the overall identified abrupt coolings are well correlated with Heinrich-type events previously recorded on the Iberian margin as well as with Heinrich events identified from North Atlantic records within the Ruddiman IRD belt, thus reinforcing the use of coccolithophore assemblage analyses for identification of millennial-scale climate variability related to Northern Hemisphere ice-sheet instability.

Acknowledgments

This research used samples provided by the Integrated Ocean Drilling Program (IODP), Exp 339. The study was financially supported by Università di Bari Aldo Moro: Fondi di Ateneo, M. Marino, 2012. The microscope laboratory at the Dipartimento di Scienze della Terra and Geoambientali, University of Bari Aldo Moro, was funded by Potenziamento Strutturale PONa3_00369 "Laboratorio per lo Sviluppo Integrato delle Scienze e delle Tecnologie dei Materiali Avanzati e per dispositivi innovativi (SISTEMA)". T. Rodrigues thanks the Fundação para a Ciência e a Tecnologia (FCT) through the post-doctoral fellowships (SFRH/BPD/66025/2009); funding for C_{37} alkenones analyses provided by the CLIMHOL project (PDCT/MAR/100157/2008) and DiatBio (PTDC/AAG-GLO/3737/2012). Financial support from IODP PEA and UCSC Silicon Valley Initiatives (SVI) Research Award to B. Balestra and from the project CTM2012-

38248 (VACLIODP339), Ministerio de Economía y Competitividad (Spain) to J.-A. Flores are also acknowledged.

Appendix A

The ecological behavior of few coccolithophore taxa and their use as proxy of surface water modification as adopted in the present paper are reported below.

A.1. Warm-water taxa

The cumulative abundances of the warm water taxa (wwt group) *Umbilicosphaera sibogae* ssp. *sibogae* and *Umbilicosphaera sibogae* ssp. *foliosa*, *Rhabdosphaera clavigera*, *Calciosolenia* spp., *Oolithotus* spp. (mostly *Oolithotus antillarum*), and *Umbellosphaera* spp., are considered as warm water proxy at Site U1385. The distinctive increases of the wwt curve can be considered as indicator of warmer and oligotrophic surface water as well (McIntyre and Bè, 1967; Winter et al., 1994; Ziveri et al., 2004; Baumann et al., 2004; Boeckel and Baumann, 2004; Saavedra-Pellitero et al., 2010; Palumbo et al., 2013). Within this group, the pattern of *Umbellosphaera* spp., mainly composed by *Umbellosphaera tenuis* and *Umbellosphaera irregularis*, is also used to infer well-developed oligotrophic conditions from the surface down to the middle of the photic zone (Kinkel et al., 2000; Okada and McIntyre, 1979). High abundances of living *Umbellosphaera* spp. (up to 70% of the assemblages) were in fact recorded at intermediate depth (50–100 m) in oligotrophic waters of the equatorial Atlantic (Kinkel et al., 2000). In particular *Umbellosphaera tenuis* seems to indicate lower light intensity surface waters usually between 50 m and 75 m water depth (Cortes et al., 2001). On the other hand *U. irregularis* is considered one of the most oligotrophic coccolithophore species (Cortes et al., 2001).

A.2. F. profunda

Increased abundances of *F. profunda* can be considered as proxy of seasonal stratification, lower surface water productivity, and deep nutricline (Molfino and McIntyre, 1990a,b; McIntyre and Molfino, 1996; Beaufort et al., 1997; Henriksson, 2000). In addition, this species is a deep dwelling taxon and because of its minimum temperature limit of about 10–12 °C (Okada and Honjo, 1973), may also provide information about conditions near the thermocline.

Increased abundances of the taxon during HE (Colmenero-Hidalgo et al., 2004) have been related to both high turbidity in the upper photic zone/decreased light intensity that forced *F. profunda* to migrate upwards (Ahagon et al., 1993) and to stratification in the upper photic zone and a deepening of the nutricline (Molfino and McIntyre, 1990a,b).

A.3. C. pelagicus ssp. pelagicus

C. pelagicus ssp. *pelagicus* is used as a proxy of polar-subpolar melt-water influx at the site location. The taxon is considered a subarctic species (Baumann et al., 2000; Geisen et al., 2002) which dwells in colder condition (Okada and McIntyre, 1979; Winter et al., 1994) recording prominent increases during Heinrich type events in the west part of the Iberian margin within MIS 12 (core MD03-2699, Amore et al., 2012) and within glacials of MB interval (core MD01-2446, Marino et al., 2014). In surface waters off Western Iberia (Parente et al., 2004) *C. pelagicus* ssp. *pelagicus* co-occurs with high abundances of *Neogloboquarina pachyderma* left coiling, a polar–subpolar taxon (Hemleben et al., 1989; Johannessen et al., 1994), during Heinrich events of the last 200 kyr, supporting a clear relation with influx of subpolar water in this mid-latitude North Atlantic region. A similar pattern of *C. pelagicus* ssp. *pelagicus*, showing sharp increases close to IRD peaks, has been recorded at the northern Atlantic ODP Site 980 during the mid-Pleistocene (Marino et al., 2011).

A.4. G. margereli–G. muellerae

The higher occurrence of *G. margereli–G. muellerae* is a proxy of glacial condition since the taxon is a cool-cold surface water indicator, in agreement with data from many ocean records. Modern *G. muellerae* is in fact mainly recorded in the eastern North Atlantic, north of 50°N and south of the Iceland-Scotland Ridge (10–30°W) (Giraudeau et al., 2010; Balestra et al., 2010) and it is considered a cold taxon (Weaver and Pujol, 1988; Samtleben and Bickert, 1990; Bollmann, 1997; Okada and Wells, 1997; Saavedra-Pellitero et al., 2010; Amore et al., 2012). *G. margereli* is the representative gephyrocapsid of transitional coccolithophore assemblages (Bollmann, 1997). *G. margereli–G. muellerae* > 4 μm, which records significant occurrence in MB glacials starting from MIS 12 in North Atlantic (Marino et al., 2014) and Mediterranean Sea (Girone et al., 2013), is used as a signal of colder and low-salinity water influx at the site location possibly linked to abrupt glacial episodes of iceberg melting.

References

Abrantes, F., Moita, T., 1999. Water column and recent sediment data on diatoms and coccolithophorids, off Portugal, confirm sediment record of upwelling events. Oceanol. Acta 22 (3), 319–336.

Adkins, J.F., Ingersoll, A.P., Pasquero, C., 2005. Rapid climate change and conditional instability of the glacial deep ocean from the thermobaric effect and geothermal heating. Quat. Sci. Rev. 24, 581–594.

Ahagon, N., Tanaka, Y., Ujiié, H., 1993. Florisphaera profunda, a possible nannoplankton indicator of late Quaternary changes in sea-water turbidity at the northwestern margin of the Pacific. Mar. Micropaleontol. 22 (3), 255–273.

Alonso-Garcia, M., Sierro, F.J., Flores, J.A., 2011. Arctic front shifts in the subpolar North Atlantic during the Mid-Pleistocene (800–400 ka) and their implications for ocean circulation. Palaeogeogr. Palaeoclimatol. Palaeoecol. 311 (3-4), 268–280. http://dx.doi.org/10.1016/j.palaeo.2011.09.004.

Amore, F.O., Flores, J.A., Voelker, A.H.L., Lebreiro, S.M., Palumbo, E., Sierro, F.J., 2012. A Middle Pleistocene Northeast Atlantic coccolithophore record: paleoclimatology and paleoproductivity aspects. Mar. Micropaleontol. 90–91, 44–59.

Balch, W.M., 2004. Re-evaluation of the physiological ecology of coccolithophores. In: Thierstein, H.R., Young, J.R. (Eds.), Coccolithophores: From Molecular Processes to Global Impact. Springer-Verlag, Berlin, pp. 165–190.

Balestra, B., Ziveri, P., Baumann, K.-H., Monechi, S., Troelstra, S., 2010. Surface water dynamics in the Reykjanes Ridge area during the Holocene as revealed by coccolith assemblages. Mar. Micropaleontol. 76, 1–10.

Balestra, B., Flores, J.-A., Hodell, D., Hernández-Molina, F.J., Stow, D.A.V., 2015. Pleistocene calcareous nannofossil biochronology at IODP Site U1385 (Exp 339). Glob. Planet. Chang. (in this issue).

Bard, E., Rostek, F., Turon, J.L., Gendreau, S., 2000. Hydrological impact of Heinrich events in the subtropical northeast Atlantic. Science 289, 1321–1324.

Barker, S., Archer, D., Booth, L., Elderfield, H., Henderiks, J., Rickaby, R.E.M., 2006. Globally increased pelagic carbonate production during the Mid-Brunhes Dissolution Interval and the CO_2 paradox of MIS 11. Quat. Sci. Rev. 25, 3278–3293.

Barker, S., Knorr, G., Edwards, R.L., Rarrenin, F., Putnam, A.E., Skinner, L.C., Wolff, E., Ziegler, M., 2011. 800,000 years of abrupt climate variability. Science 334, 347–351.

Bassinot, F.C., Labeyrie, L.D., Vincent, E., Quidelleur, X., Shackleton, N.J., Lancelot, Y., 1994. The astronomical theory of climate and the age of the Brunhes–Matuyama magnetic reversal. Earth Planet. Sci. Lett. 126, 91–108.

Baumann, K.-H., Freitag, T., 2004. Pleistocene fluctuations in the northern Benguela Current system as revealed by coccolith assemblages. Mar. Micropaleontol. 52, 195–215.

Baumann, K.-H., Andruleit, H., Samtleben, C., 2000. Coccolithophores in the Nordic Seas: comparison of living communities with surface sediment assemblages. Deep-Sea Res. II 47, 1743–1772.

Baumann, K.-H., Bockel, B., Frenz, M., 2004. Coccolith contribution to South Atlantic carbonate sedimentation. In: Thierstein, H.R., Young, J. (Eds.), Coccolithophores, from Molecular Processes to Global Impact. Springer, Berlin, pp. 367–402.

Baumann, K.H., Andruleit, H., Böckel, B., Geisen, M., Kinkel, H., 2005. The significance of extant coccolithophores as indicators of ocean water masses, surface water temperature, and paleoproductivity: a review. Paläontol. Z. 79, 93–112.

Beaufort, L., Lancelot, Y., Camberlin, P., Cayre, O., Vincent, E., Bassinot, F., Labeyrie, L., 1997. Insolation cycles as a major control of Equatorial Indian Ocean primary production. Science 278, 1451–1454.

Berger, W.H., Jansen, E., 1994. Mid-Pleistocene climate shift: the Nansen connection. In: Johannessen, O.M., Muensch, R.D., Overland, J.E. (Eds.), The Role of the Polar Oceans in Shaping the Global Environment. Geophys. Monogr. Am. Geophys. Union 85, pp. 295–311.

Billups, K., Lindley, C., Fisler, J., Martin, P., 2006. Mid Pleistocene climate instability in the subtropical northwestern Atlantic. Global Planet. Change 54 (3–4), 251–262. http://dx.doi.org/10.1016/j.gloplacha.2006.06.025.

Bintanja, R., van de Wal, R.S.W., 2008. North American ice-sheet dynamics and the onset of 100,000-year glacial cycles. Nature 454, 869–872. http://dx.doi.org/10.1038/nature07158.

Boeckel, B., Baumann, K.-H., 2004. Distribution of coccoliths in surface sediments of the south-eastern South Atlantic Ocean: ecology, preservation and carbonate contribution. Mar. Micropaleontol. 51, 3101–3320.

Bollmann, J., 1997. Morphology and biogeography of *Gephyrocapsa* coccoliths in Holocene sediments. Mar. Micropaleontol. 29, 319–350.

Bollmann, J., Baumann, K.-H., Thierstein, H.R., 1998. Global dominance of *Gephyrocapsa* coccoliths in the late Pleistocene: Selective dissolution, evolution, or global environmental change? Paleoceanography 13 (5), 517–529.

Bowen, D.Q., 2010. Sea level 400000 years ago (MIS 11): analogue for present and future sea-level? Clim. Past 6, 10–29.

Brand, L.E., 1994. Physiological ecology of marine coccolithophores. In: Siesser, W.G., Winter, A. (Eds.), Coccolithophores. Cambridge University Press, pp. 39–49.

Broecker, W.S., Bond, G., McManus, J.F., Klas, M., Clark, E., 1992. Origin of the northern Atlantic's Heinrich events. Clim. Dyn. 6, 265–273.

Candy, I., McClymont, E.L., 2013. Interglacial intensity in the North Atlantic over the last 800 000 years: investigating the complexity of the mid-Brunhes Event. J. Quat. Sci. 28 (4), 343–348.

Channell, J.E.T., Hodell, D.A., Romero, O., Hillaire-Marcel, C., de Vernal, A., Stoner, J.S., Mazaud, A., Röhl, U., 2012. A 750-kyr detrital-layer stratigraphy for the North Atlantic (IODP Sites U1302–U1303, Orphan Knoll, Labrador Sea). Earth Planet. Sci. Lett. 317–318, 218–230. http://dx.doi.org/10.1016/j.epsl.2011.11.029.

Clark, P.U., Archer, D., Pollard, D., Blum, J.D., Rial, J.A., Brovkin, V., Mix, A.C., Pisias, N.G., Roy, M., 2006. The middle Pleistocene transition: characteristics, mechanisms, and implications for long-term changes in atmospheric CO_2. Quat. Sci. Rev. 25, 3150–3184.

Colmenero-Hidalgo, E., Flores, J.A., Sierro, F.J., Barcena, M.A., Lowemark, L., Schonfeld, J., Grimalt, J.O., 2004. Ocean surface water response to short-term climate changes revealed by coccolithophores from the Gulf of Cadiz (NE Atlantic) and Alboran Sea (W Mediterranean). Palaeogeogr. Palaeoclimatol. Palaeoecol. 205, 317–336.

Cortes, M., Bollmann, J., Thierstein, H.R., 2001. Coccolithophore ecology at the HOT station ALOHA Hawaii. Deep-Sea Res. II 48, 1947–1981.

Crowley, T.J., 1985. Late Quaternary carbonate changes in the North Atlantic and Atlantic/Pacific comparisons. In: Sundquist, E., Broecker, W.S. (Eds.), The Carbon Cycle and Atmospheric CO_2: Natural Variations Archean to PresentGeophysical Monograph Series.AGU, Washington, DC, pp. 271–284.

Curry, W.B., Oppo, D.W., 2005. Glacial water mass geometry and the distribution of delta C-13 of Sigma CO2 in the western Atlantic Ocean. Paleoceanography 20, PA1017. http://dx.doi.org/10.1029/2004PA001021.

Dansgaard, W., Johnsen, S.J., Clausen, H.B., Dahl-Jensen, D., Gunderstrup, N.S., Hammer, C.V., Hvidberg, C.S., Steffensen, J.P., Sveinbjornsdottir, A.E., Jouzel, J., Bard, G., 1993. Evidence for general instability of past climate from a 250 kyr ice-core record. Nature 364, 218–220.

de Abreu, L., Shackleton, N.J., Schonfeld, J., Hall, M., Chapman, M., 2003. Millennial scale oceanic climate variability off the western Iberian margin during the last two glacial periods. Mar. Geol. 196, 1–20.

de Abreu, L., Abrantes, F., Shackleton, N., Tzedakis, P.C., McManus, J.F., Oppo, D.W., Hall, M.A., 2005. Ocean climate variability in the eastern North Atlantic during interglacial marine isotope stage 11: a partial analogue for the Holocene? Paleoceanography 20, PA3009. http://dx.doi.org/10.1029/2004PA001091.

Desprat, S., Sánchez Goñi, M.F., Turon, J.-L., McManus, J.F., Loutre, M.F., Duprat, J., Malaizé, B., Peyron, O., Peypouquet, J.-P., 2005. Is vegetation responsible for glacial inception during periods of muted insolation changes? Quat. Sci. Rev. 24, 1361–1374.

Dittert, N., Baumann, K.-H., Bickert, R., Henrich, R., Huber, R., Kinkel, H., Meggers, H., 1999. Carbonate dissolution in the deep-sea: methods, quantification and paleoceanographic application. In: Fischer, G., Wefer, G. (Eds.), Use of Proxies in Paleoceanography: Examples from the South Atlantic. Springer Verlag, Berlin, Heidelberg, pp. 255–284.

Droxler, A.W., Farrell, J.W., 2000. Marine Isotope Stage 11 (MIS 11): new insights for a warmer future. Glob. Planet. Chang. 24, 1–5.

Droxler, A.W., Morse, J.W., Kornicker, W.A., 1988. Controls on carbonate mineral accumulation in Bahamian basins and adjacent Atlantic Ocean sediments. J. Sediment. Petrol. 58, 120–130.

Droxler, A.W., Ferro, E.C., Mucciarone, D.A., Haddad, G.A., 1997. The marine carbonate system during oxygen isotope stage 11 (423–362 ka): a case of basin-to-shelf and/or basin-to-basin carbonate fractionation? EOS Trans. Am. Geophys. Union 78, S179.

EPICA community members, 2004. Eight glacial cycles from an Antarctic ice core. Nature 429, 623–628.

Expedition 339 Scientists, 2013. Site U1385. In: Stow, D.A.V., Hernández-Molina, F.J., Alvarez Zarikian, C.A., Expedition 339 Scientists (Eds.), Proc. IODP 339. Integrated Ocean Drilling Program Management International, Inc., Tokyo. http://dx.doi.org/10.2204/iodp.proc.339.103.2013.

Eynaud, F., de Abreu, L., Voelker, A., Schönfeld, J., Salgueiro, E., Turon, J.-L., Penaud, A., Toucanne, S., Naughton, F., Sanchez Goñi, M.F., Malaizé, B., Cacho, I., 2009. Position of the Polar Front along the western Iberian margin during key cold episodes of the last 45 ka. Geochem. Geophys. Geosyst. 10, Q07U05. http://dx.doi.org/10.1029/2009GC002398.

Fiúza, A.F.G., 1984. Hidrologia e dinámica das águas costeiras de Portugal (Ph.D. thesis) Univ. of Lisbon, Lisbon.

Fiúza, A., Macedo, M., Guerreiro, M., 1982. Climatological space and time variation of the Portuguese coastal upwelling. Oceanologica Acta 5, 31–40.

Fiúza, A.F.G., Hamann, M., Ambar, I., Díaz del Río, G., González, N., Cabanas, J.M., 1998. Water masses and their circulation off western Iberia during May 1993. Deep-Sea Res. I Oceanogr. Res. Pap. 45, 1127–1160.

Flores, J.A., Sierro, F.J., 1997. Revised technique for calculation of calcareous nannofossil accumulation rates. Micropaleontology 43, 321–324.

Flores, J.A., Gersonde, R., Sierro, F.J., 1999. Pleistocene fluctuations in the Agulhas current retroflection based on the calcareous plankton record. Mar. Micropaleontol. 37, 1–22.

Flores, J.A., Marino, M., Sierro, F.J., Hodell, D.A., Charles, C.D., 2003. Calcareous plankton dissolution pattern and coccolithophore assemblages during the last 600 kyr at ODP Site 1089 (Cape Basin, South Atlantic): paleoceanographic implications. Palaeogeogr. Palaeoclimatol. Palaeoecol. 196, 409–426.

Flores, J.-A., Sierro, F.J., Filippelli, G., Bárcena, M., Pérez-Folgado, M., Vásquez, A., Utrilla, R., 2005. Surface water dynamics and phytoplankton communities during deposition of cyclic late Messinian sapropel sequences in the western Mediterranean. Mar. Micropaleontol. 56, 50–79.

Frouin, R., Fiúza, A., Ambar, I., Boyd, T.J., 1990. Observations of a poleward surface current off the coasts of Portugal and Spain during the winter. J. Geophys. Res. 95, 679–691.

Gartner, S., 1988. Paleoceanography of the Mid-Pleistocene. Mar. Micropaleontol. 13, 23–46.

Gartner, S., Chow, J., Stanton, R.J., 1987. Late Neogene paleoceanography of the eastern Caribbean, the Gulf of Mexico, and the eastern Equatorial Pacific. Mar. Micropaleontol. 12 (3), 255–304.

Geisen, M., Billard, C., Broerse, A.T.C., Cros, L., Probert, I., Young, J.R., 2002. Life-cycle associations involving pairs of holococcolithophorid species: intraspecific variation or cryptic speciation? Eur. J. Phycol. 37, 531–550.

Giraudeau, J., 1992. Distribution of recent nannofossils beneath the Benguela system: southwest African continental margin. Mar. Geol. 108, 219–237.

Giraudeau, J., Grelaud, M., Solignac, S.J., Andrews, T., Moros, M., Jansen, E., 2010. Millennial-scale variability in Atlantic water advection to the Nordic Seas derived from Holocene coccolith concentration records. Quat. Sci. Rev. 29, 1276–1287.

Girone, A., Maiorano, P., Marino, M., Kucera, M., 2013. Calcareous plankton response to orbital and millennial-scale climate changes across the Middle Pleistocene in the western Mediterranean. Palaeogeogr. Palaeoclimatol. Palaeoecol. 392, 105–116. http://dx.doi.org/10.1016/j.palaeo.2013.09.005.

Grelaud, M., Beaufort, L., Cuven, S., Buchet, N., 2009. Glacial to interglacial primary production and El Niño–Southern Oscillation dynamics inferred from coccolithophores of the Santa Barbara Basin. Paleoceanography 24. http://dx.doi.org/10.1029/2007PA001578.

Hagino, K., Kulhanek, D.K., 2009. Data report: calcareous nannofossils from upper Pliocene and Pleistocene, Expedition 306 Sites U1313 and U1314. In: Channell, J.E.T., Kanamatsu, T., Sato, T., Stein, R., Alvarez Zarikian, C.A., Malone, M.J., Expedition 303/306 Scientists (Eds.), Proceedings of the Integrated Ocean Drilling Program 303/306. College Station, TX., USA.

Haynes, R., Barton, E.D., 1990. A poleward flow along the Atlantic coast of the Iberian Peninsula. J. Geophys. Res. 95, 11425–11442.

Hearty, P.J., Kindler, P., Cheng, H., Edwards, R.L., 1999. A + 20 m middle Pleistocene sea-level highstand (Bermuda and the Bahamas) due to partial collapse of Antarctic ice. Geology 27, 375–378.

Heinrich, H., 1988. Origin and consequences of cyclic ice rafting in the northeast Atlantic Ocean during the past 130,000 years. Quat. Res. 29, 142–152.

Helmke, J.P., Bauch, H.A., Röhl, U., Kandiano, E.S., 2008. Uniform climate development between the subtropical and subpolar Northeast Atlantic across marine isotope stage 11. Clim. Past Discuss. 4, 433–457.

Hemleben, C., Spindler, M., Anderson, O.R., 1989. Modern Planktonic Foraminifera. Springer-Verlag, New York.

Hemming, S.R., 2004. Heinrich events: massive late Pleistocene detritus layers of the North Atlantic and their global climate imprint. Rev. Geophys. 42. http://dx.doi.org/10.1029/2003RG000128.

Henriksson, A.S., 2000. Coccolithophore response to oceanographic changes in the equatorial Atlantic during the last 200,000 years. Palaeogeogr. Palaeoclimatol. Palaeoecol. 156, 161–173. http://dx.doi.org/10.1016/S0031-0182(99)00139-X.

Hine, N.M., Weaver, P.P.E., 1998. Quaternary. In: Brown, P.R. (Ed.), Calcareous Nannofossil BiostratigraphyBritish Micropalaeontology Society Series. Chapman & Hall, London, pp. 266–283.

Hodell, D.A., Charles, C.D., Ninneman, U.S., 2000. Comparison of interglacial stages in the South Atlantic sector of the southern ocean for the past 450 ka: implications for marine isotope stage (MIS) 11. Glob. Planet. Chang. 24 (1), 7–26.

Hodell, D.A., Venz, K.A., Charles, C.D., Ninnemann, U.S., 2003. Pleistocene vertical isotope and carbonate gradient in South Atlantic sector of the Southern Ocean. Geochem. Geophys. Geosyst. 4, 1004. http://dx.doi.org/10.1020/2002GC000367.

Hodell, D.A., Channell, J.E.T., Curtis, J.H., Romero, O.E., Röhl, U., 2008. Onset of "Hudson Strait" Heinrich Events in the Eastern North Atlantic at the end of the Middle Pleistocene Transition (−640 ka)? Paleoceanography 23, PA4218. http://dx.doi.org/10.1029/2008PA001591.

Hodell, D.A., Lourens, L., Stow, D.A.V., Hernández-Molina, J., Alvarez Zarikian, C.A., Shackleton Site Project Members, 2013a. The "Shackleton Site" (IODP Site U1385) on the Iberian Margin. Sci. Drill. 16, 13–19. http://dx.doi.org/10.5194/sd-16-13-2013 (www.sci-dril.net/16/13/2013/).

Hodell, D.A., Crowhurst, S., Skinner, L., Tzedakis, P.C., Margari, V., Channell, J.E.T., Kamenov, G., Maclachlan, S., Rothwell, G., 2013b. Response of Iberian Margin sediments to orbital and suborbital forcing over the past 420 ka. Paleoceanography 28 (1–15), 2013. http://dx.doi.org/10.1002/palo.20017.

Hodell, D., Lourens, L., Crowhurst, S., Konijnendijk, T., Tjallingii, R., Jiminez-Espejo, F., Tzedakis, P.C., Skinner, L., Shackleton Site Project Members, 2015. A reference time scale for Site U1385 (Shackleton Site) on the Iberian Margin. Glob. Planet. Chang. (in this issue).

Honjo, S., Okada, H., 1974. Community structure of coccolithophores in the photic layer of the mid-Pacific. Micropaleontology 20, 209–230.

Howard, W., 1997. A warm future in the past. Nature 388, 418–419.

Howard, W.R., Prell, W.L., 1994. Late Quaternary $CaCO_3$ production and preservation in the Southern Ocean: implications for oceanic and atmospheric carbon cycling. Paleoceanography 9 (3), 453–482. http://dx.doi.org/10.1029/93PA03524.

Incarbona, A., Martrat, B., Di Stefano, E., Grimalt, J.O., Pelosi, N., Patti, B., Tranchida, G., 2010. Primary productivity variability on the Atlantic Iberian Margin over the last 70,000 years: evidence from coccolithophores and fossil organic compounds. Paleoceanography 25, PA2218. http://dx.doi.org/10.1029/2008PA001709.

Jansen, J.H.F., Kuijpers, A., Troelstra, S.R., 1986. A mid-Brunhes climatic event: long-term changes in global atmospheric and ocean circulation. Science 232, 619–622.

Ji, J., Ge, Y., Balsam, W., Damuth, J.E., Chen, J., 2009. Rapid identification of dolomite using a Fourier transform infrared spectrophotometer (FTIR): a fast method for identifying Heinrich events in IODP Site U1308. Mar. Geol. 258, 60–68.

Johannessen, T., Jansen, E., Flatoy, A., Ravelo, A.C., 1994. The relationship between surface water masses, oceanographic fronts and paleoclimatic proxies in surface sediments of the Greenland Iceland and Norwegian seas. In: Zahn, R., Pedersen, T.F., Kaminski, M.A., Labeyrie, L. (Eds.), Carbon Cycling in the Glacial Ocean: Constraints on the Ocean's Role in Global ChangeNATO Asi Series I 17. Springer, New York, USA, pp. 61–85.

Jouzel, J., Masson-Delmotte, V., Cattani, O., Dreyfus, G., Falourd, S., Hoffmann, G., Minster, B., Nouet, J., Barnola, J.M., Chappellaz, J., Fischer, H., Gallet, J.C., Johnsen, S., Leuenberger, M., Loulergue, L., Luethi, D., Oerter, H., Parrenin, F., Raisbeck, G., Raynaud, D., Schilt, A., Schwander, J., Selmo, E., Souchez, R., Spahni, R., Stauffer, B., Steffensen, J.P., Stenni, B., Stocker, T.F., Tison, J.L., Werner, M., Wolff, E.W., 2007. Orbital and millennial Antarctic climate variability over the past 800,000 years. Science 317, 793–796.

Kandiano, E.S., Bauch, H.A., Fahl, K., Helmke, J.P., Röhl, U., Pérez-Folgado, M., Cacho, I., 2012. The meridional temperature gradient in the eastern North Atlantic during MIS11 and its link to the ocean–atmosphere system. Palaeogeogr. Palaeoclimatol. Palaeoecol. 333–334, 24–39.

Kindler, P., Hearty, P.J., 2000. Elevated marine terraces from Eleuthera (Bahamas) and Bermuda: sedimentological, petrographic, and geochronological evidence for important deglaciation events during the middle Pleistocene. Glob. Planet. Chang. 24, 41–58.

Kinkel, H., Baumann, K.-H., Čepek, M., 2000. Coccolithophores in the equatorial Atlantic Ocean: response to seasonal and late Pleistocene surface water variability. Mar. Micropaleontol. 39, 87–112.

Kleijne, A., 1990. Distribution and malformation of extant calcareous nannoplankton in the Indonesian seas. Mar. Micropaleontol. 16, 293–316.

Lang, N., Wolff, E.W., 2011. Interglacial and glacial variability from the last 800 ka in marine, ice and terrestrial archives. Clim. Past 7, 361–380. http://dx.doi.org/10.5194/cp-7-361-2011.

Laskar, J., Robutel, P., Joutel, F., Gastineau, M., Correia, A.C.M., Levrard, B., 2004. A long-term numerical solution of the insolation quantities of the Earth. Astron. Astrophys. 428, 261–285.

Lebreiro, S.M., Moreno, J.C., McCave, I.N., Weaver, P.P.E., 1996. Evidence for Heinrich layers off Portugal (Tore Seamount: 39°N, 12°W). Mar. Geol. 131, 47–56.

Lebreiro, S.M., Voelker, A.H.L., Vizcaino, A., Abrantes, F., Alt-Epping, U., Jung, S., Thouveny, N., Gràcia, E., 2009. Sediment instability on the Portuguese continental margin under abrupt glacial climate changes (last 60 kyr). Quat. Sci. Rev. 28 (27-28), 3211–3223. http://dx.doi.org/10.1016/j.quascirev.2009.08.007.

Lisiecki, L.E., Raymo, M.E., 2005. A Pliocene–Pleistocene stack of 57 globally distributed benthic $\delta^{18}O$ records. Paleoceanography 20, PA1003. http://dx.doi.org/10.1029/2004PA001071.

Lopez-Otalvaro, G.E., Flores, J.A., Sierro, F.J., Cacho, I., 2008. Variations in coccolithophorid production in the Eastern Equatorial Pacific at ODP Site 1240 over the last seven glacial–interglacial cycles. Mar. Micropaleontol. 69, 52–69.

Maiorano, P., Tarantino, F., Marino, M., De Lange, G.J., 2013. Paleoenvironmental conditions at Core KC01B (Ionian Sea) through MIS 13-9: Evidence from calcareous nannofossil assemblages. Quat. Int. 288, 97–111.

Margari, V., Skinner, L.C., Tzedakis, P.C., Ganopolski, A., Vautravers, M., Shackleton, N.J., 2010. The nature of millennial-scale climate variability during the past two glacial periods. Nat. Geosci. 3, 127–131.

Marino, M., Maiorano, P., Flower, B.P., 2011. Calcareous nannofossil changes during the Mid-Pleistocene Revolution: Paleoecologic and paleoceanographic evidence from North Atlantic Site 980/981. Palaeogeogr. Palaeoclimatol. Palaeoecol. 306, 58–69.

Marino, M., Maiorano, P., Tarantino, F., Voelker, A., Capotondi, L., Girone, A., Lirer, F., Flores, J.-A., Naafs, B.D.A., 2014. Coccolithophores as proxy of seawater changes at orbital-to-millennial scale during middle Pleistocene Marine Isotope Stages 14–9 in North Atlantic core MD01-2446. Paleoceanography 29. http://dx.doi.org/10.1002/2013PA002574.

Martrat, B., Grimalt, J.O., Shackleton, N.J., De Abreu, L., Hutterli, M.A., Stocker, T.F., 2007. Four climate cycles of recurring deep and surface water destabilizations on the Iberian margin. Science 317, 502–507. http://dx.doi.org/10.1126/science.1139994.

Maslin, M.A., Shackleton, N.J., Pflaumann, U., 1995. Surface water temperature, salinity, and density changes in the northeast Atlantic during the last 45,000 years: Heinrich events, deep water formation, and climatic rebounds. Paleoceanography 10. http://dx.doi.org/10.1029/94PA03040.

Mayer, L., Pisias, N., Janecek, T., Scientific Party, Shipboard, 1992. Explanatory notes. In: Mayer, L., Pisias, N., Janecek, T., et al. (Eds.), Proc. ODP, Init. Repts. 138. Ocean Drilling Program, College Station, TX, pp. 13–42

McCartney, M.S., Talley, L.D., 1982. The Subpolar Mode Water of the North Atlantic Ocean. J. Phys. Oceanogr. 12, 1169–1188.

McIntyre, A., Bè, A.H.W., 1967. Modern coccolithophores of the Atlantic Ocean — I. Placolith and cyrtoliths. Deep-Sea Res. 14, 561–597.

McIntyre, A., Molfino, B., 1996. Forcing of Atlantic equatorial and subpolar millennial cycles by precession. Science 274, 1867–1870. http://dx.doi.org/10.1126/science.274.5294.1867.

McManus, J.F., Oppo, D.W., Cullen, J.L., 1999. A 0.5 million year record of millennial-scale climate variability in the North Atlantic. Science 283 (5404), 971–975. http://dx.doi.org/10.1126/science.283.5404.971.

McManus, J.F., Francois, R., Gherardi, J.-M., Keigwin, L.D., Brown-Leger, S., 2004. Collapse and rapid resumption of Atlantic meridional circulation linked to deglacial climate changes. Nature 428, 834–837.

Milker, Y., Rachmayani, R., Weinkauf, M., Prange, M., Raitzsch, M., Schulz, M., Kucera, M., 2013. Global and regional sea surface temperature trends during Marine Isotope Stage 11. Clim. Past 837–890 (Discussions 9).

Mitchell-Innes, B.A., Winter, A., 1987. Coccolithophores: a major phytoplankton component in mature upwelled water off the Cape Peninsula, South Africa in March, 1983. Mar. Biol. 95, 25–30.

Mix, A.C., Pisias, N.G., Rugh, W., Wilson, J., Morey, A., Hagelberg, T.K., 1995. Benthic foraminifer stable isotope record from Site 849, (0-5 Ma): local and global climate changes. Proc. Ocean Drill. Program Sci. Results 138, 371–412.

Moita, T., 1993. Spatial variability of phytoplankton communities in the upwelling region off Portugal. Proceeding of the International Council for the Exploration of the Sea, L64, Copenhagen, Denmark, pp. 1–2.

Moita, M.T., Silva, A., Palma, S., Vilarinho, M.G., 2010. The coccolithophore summer–autumn assemblage in the upwelling waters of Portugal: patterns of mesoscale distribution (1985–2005). Estuar. Coast. Shelf Sci. 87, 411–419.

Molfino, B., McIntyre, A., 1990a. Precessional forcing of nutricline dynamics in the Equatorial Atlantic. Science 249, 766–769.

Molfino, B., McIntyre, A., 1990b. Nutricline variation in the equatorial Atlantic coincident with the Younger Dryas. Paleoceanography 5, 997–1008.

Moreno, E., Thouveny, N., Delanghe, D., McCave, I.N., Shackleton, N.J., 2002. Climatic and oceanographic changes in the Northeast Atlantic reflected by magnetic properties of sediments deposited on the Portuguese margin during the last 340 ka. Earth Planet. Sci. Lett. 202 (2), 465–480. http://dx.doi.org/10.1016/S0012-821X(02)00787-2.

Mudelsee, M., Schulz, M., 1997. The mid-Pleistocene climate transition: onset of 100 ka cycle lags ice volume build-up by 280 ka. Earth Planet. Sci. Lett. 151, 117–123.

Naafs, B.D.A., Hefter, J., Ferretti, P., Stein, R., Haug, G.H., 2011. Sea surface temperatures did not control the first occurrence of Hudson Strait Heinrich Events during MIS 16. Paleoceanography 26, PA4201. http://dx.doi.org/10.1029/2011PA002135.

Naafs, B.D.A., Hefter, J., Stein, R., 2013. Millennial-scale ice rafting events and Hudson Strait Heinrich(-like) Events during the late Pliocene and Pleistocene: a review. Quat. Sci. Rev. 80, 1–28. http://dx.doi.org/10.1016/j.quascirev.2013.08.014.

Naughton, F., Sánchez Goñi, M.F., Kageyama, M., Bard, E., Duprat, J., Cortijo, E., Desprat, S., Malaizé, B., Joly, C., Rostek, F., Turon, J.-L., 2009. Wet to dry climatic trend in north-western Iberia within Heinrich events. Earth Planet. Sci. Lett. 284 (1–2), 329–342.

Okada, H., Honjo, S., 1973. The distribution of oceanic coccolithophorids in the Pacific. Deep-Sea Res. 20, 355–374.

Okada, H., McIntyre, A., 1979. Seasonal distribution of modern coccolithophores in the western North Atlantic Ocean. Mar. Biol. 54, 319–328.

Okada, H., Wells, P., 1997. Late Quaternary nannofossil indicators of climate change in two deep-sea cores associated with the Leeuwin Current off Western Australia. Palaeogeogr. Palaeoclimatol. Palaeoecol. 131, 413–432.

Oppo, D.W., McManus, J., Cullen, J.C., 1998. Abrupt climate change events 500 000 to 340 000 years ago: evidence from subpolar North Atlantic sediments. Science 279, 1335–1338.

Pailler, D., Bard, E., 2002. High frequency palaeoceanographic changes during the past 140000 yr recorded by the organic matter in sediments of the Iberian Margin. Palaeogeogr. Palaeoclimatol. Palaeoecol. 181 (4), 431–452. http://dx.doi.org/10.1016/S0031-0182(01)00444-8.

Palumbo, E., Flores, J.A., Perugia, C., Petrillo, Z., Voelker, A.H.L., Amore, F.O., 2013. Millennial scale coccolithophore paleoproductivity and surface water changes between 445 and 360 ka (Marine Isotope Stages 12/11) in the Northeast Atlantic. Palaeogeogr. Palaeoclimatol. Palaeoecol. 383–384, 27–41.

Parente, A., Cachão, M., Baumann, K.-H., de Abreu, L., Ferreira, J., 2004. Morphometry of Coccolithus pelagicus s.l. (Coccolithophore, Haptophyta) from offshore Portugal, during the last 200 kyr. Micropaleontology 50, 107–120.

Peliz, A., Dubert, J., Santos, A.M.P., Oliveira, P.B., Le Cann, B., 2005. Winter upper ocean circulation in the Western Iberian Basin — Fronts, Eddies and Poleward Flows: an overview. Deep-Sea Res. I 52, 621–646.

Prokopenko, A.A., Karabanov, E.B., Williams, D.F., Kuzmin, M.I., Shackleton, N.J., Crowhurst, S., Peck, J.A., Gvozdkov, A.N., King, J.W., 2001. Biogenic silica record of the Lake Baikal response to climate forcing during the Brunhes. Quat. Res. 55, 123–132.

Relvas, P., Barton, E.D., Dubert, J., Oliveira, P.B., Peliz, A., da Silva, J.C.B., Santos, A.M.P., 2007. Physical oceanography of the western Iberia ecosystem: latest views and challenges. Prog. Oceanogr. 74, 149–173.

Rickaby, R.E.M., Bard, E., Sonzogni, C., Rostek, F., Beaufort, L., Barker, S., Rees, G., Schrag, D.P., 2007. Coccolith chemistry reveals secular variations in the global ocean carbon cycle? Earth Planet. Sci. Lett. 253 (1–2), 83–95.

Rodrigues, T., Voelker, A.H.L., Grimalt, J.O., Abrantes, F., Naughton, F., 2011. Iberian Margin sea surface temperature during MIS 15 to 9 (580–300 ka): glacial suborbital variability versus interglacial stability. Paleoceanography 26, PA1204. http://dx.doi.org/10.1029/2010PA001927.

Rodrigues, T., Hodell, D., Naughton, F., Abrantes, F., 2014. Paleoproductivity and paleoclimate reconstructions during present and past (MIS 11 and MIS 19). Interglacials in the SW Iberian Margin, PP53C-1244, American Geophysical Union, Fall Meeting 2014, San Francisco, USA, 15–19 December 2014.

Rohling, E.J., Grant, K., Bolshaw, M., Roberts, A.P., Siddall, M., Hemleben, Ch., Kucera, M., 2009. Antarctic temperature and global sea level closely coupled over the past five glacial cycles. Nat. Geosci. 2, 500–504.

Ruddiman, W.F., 1977. Late Quaternary deposition of ice rafted sand in the subpolar North Atlantic. Geol. Soc. Am. Bull. 83, 2817–2836.
Saavedra-Pellitero, M., Flores, J.A., Baumann, K.-H., Sierro, F.J., 2010. Coccolith distribution patterns in surface sediments of Equatorial and Southeastern Pacific Ocean. Geobios 43, 131–149. http://dx.doi.org/10.1016/j.geobios.2009.09.004.
Samtleben, C., Bickert, T., 1990. Coccoliths in sediment traps from the Norwegian Se. Mar. Micropaleontol. 16, 39–64.
Sánchez Goñi, M.F., Landais, A., Fletcher, W.J., Naughton, F., Desprat, S., Duprat, J., 2008. Contrasting impacts of Dansgaard–Oeschger events over a western European latitudinal transect modulated by orbital parameters. Quat. Sci. Rev. 27, 1136–1151.
Sánchez, R.F., Relvas, P., 2003. Spring–summer climatological circulation in the upper layer in the region of cape St. Vincent, SW Portugal. ICES J. Mar. Sci. 60, 1232–1250.
Sánchez, R.F., Relvas, P., Delgado, M., 2007. Coupled ocean wind and sea surface temperature patterns off the western Iberian Peninsula. J. Mar. Syst. 68 (1–2), 103–127. http://dx.doi.org/10.1016/j.jmarsys.2006.11.003.
Schönfeld, J., Zahn, R., De Abreu, L., 2003. Surface and deep water response to rapid climate changes at the Western Iberian Margin. Glob. Planet. Chang. 36, 237–264.
Shackleton, N.J., Hall, M.A., Vincent, E., 2000. Phase relationships between millennial-scale events 64,000–24,000 years ago. Paleoceanography 15, 565–569.
Shackleton, N.J., Fairbanks, R.G., Chiu, T.-C., Parrenin, F., 2004. Absolute calibration of the Greenland time scale: Implications for Antarctic time scales and for Δ^{14}C. Quat. Sci. Rev. 23, 1513–1522.
Silva, A., Palma, S., Moita, M.T., 2008. Coccolithophores in the upwelling waters of Portugal: four years of weekly distribution in Lisbon Bay. Cont. Shelf Res. 28, 2601–2613.
Silva, A., Palma, S., Oliveira, P.B., Moita, M.T., 2009. Composition and interannual variability of phytoplankton in a coastal upwelling region (Lisbon Bay, Portugal). J. Sea Res. 62, 238–249.
Sousa, F.M., Bricaud, A., 1992. Satellite-derived phytoplankton pigment structures in the Portuguese upwelling area. J. Geophys. Res. 97 (C7), 11343–11356.
Stein, R., Hefter, J., Grützner, J., Voelker, A., Naafs, B.D.A., 2009. Variability of surface water characteristics and Heinrich-like events in the Pleistocene midlatitude North Atlantic Ocean: biomarker and XRD records from IODP Site U1313 (MIS 16–9). Paleoceanography 24, PA2203. http://dx.doi.org/10.1029/2008PA001639.
Steinmetz, J.C., 1994. Sedimentation of coccolithophores. In: Winter, A., Siesser, W.G. (Eds.), Coccolithophores. Cambridge University Press, London, pp. 179–197.
Stolz, K., Baumann, K.H., 2010. Changes in palaeoceanography and palaeoecology during Marine Isotope Stage (MIS) 5 in the eastern North Atlantic (ODP Site 980) deduced from calcareous nannoplankton observations. Palaeogeogr. Palaeoclimatol. Palaeoecol. 292, 295–305.
Takahashi, K., Okada, H., 2000. Environmental control on the biogeography of modern coccolithophores in the southeastern Indian Ocean offshore of Western Australia. Mar. Micropaleontol. 39, 73–86.
Thomson, J., Nixon, S., Summerhayes, C.P., Schonfeld, J., Zahn, R., Grootes, P., 1999. Implications for sedimentation changes on the Iberian margin over the last two glacial/interglacial transitions from ($^{230}Th_{excess}$) o systematics. Earth Planet. Sci. Lett. 165, 255–270.
Tzedakis, P.C., Hooghiemstra, H., Palike, H., 2006. The last 1.35 million years at Tenaghi Philippon: revised chronostratigraphy and long-term vegetation trends. Quat. Sci. Rev. 25, 3416–3430.
Tzedakis, P.C., Pälike, H., Roucoux, K.H., de Abreu, L., 2009. Atmospheric methane, southern European vegetation and low–mid latitude links on orbital and millennial timescales. Earth Planet. Sci. Lett. 277, 307–317. http://dx.doi.org/10.1016/j.epsl.2008.10.027.
Vautravers, M., Shackleton, N.J., 2006. Centennial scale surface hydrology off Portugal during Marine Isotope Stage 3: insights from planktonic foraminiferal fauna variability. Paleoceanography 21, PA3004. http://dx.doi.org/10.1029/2005PA001144.
Vidal, L., Labeyrie, L., Cortijo, E., Arnold, M., Duplessy, J.C., Michel, E., Becque, S., van Weering, T.C.E., 1997. Evidence for changes in the North Atlantic Deep Water linked to meltwater surges during the Heinrich events. Earth Planet. Sci. Lett. 146, 13–27.
Villanueva, J., Grimalt, J.O., Cortijo, E., Vidal, L., Labeyrie, L., 1997. A biomarker approach to the organic matter deposited in the North Atlantic during the last climatic cycle. Geochim. Cosmochim. Acta 61, 4633–4646.
Voelker, A.H.L., de Abreu, L., Schönfeld, J., Erlenkeuser, H., Abrantes, F., 2009. Hydrographic conditions along the western Iberian margin during marine isotope stage 2. Geochem. Geophys. Geosyst. 10. http://dx.doi.org/10.1029/2009GC002605.
Voelker, A.H.L., Rodrigues, T., Billups, K., Oppo, D., McManus, J., Stein, R., Hefter, J., Grimalt, J.O., 2010. Variations in mid-latitude North Atlantic surface water properties during the mid-Brunhes (MIS 9–14) and their implications for the thermohaline circulation. Clim. Past 6, 531–552.
Volkov, D.L., Fu, L.-L., 2010. On the reasons for the existence and the variability of the Azores Current. J. Phys. Oceanogr. 40, 2197–2220. http://dx.doi.org/10.1175/2010JPO4326.1.
Wang, P., Tian, J., Cheng, X., Liu, C., Xu, J., 2003. Carbon reservoir change preceded major ice-sheet expansion at the mid-Brunhes event. Geology 31, 239–242.
Weaver, P.P.E., Pujol, C., 1988. History of the last deglaciation in the Alboran Sea (western Mediterranean) and adjacent North Atlantic as revealed by coccolith floras. Palaeogeogr. Palaeoclimatol. Palaeoecol. 64, 35–42.
Winter, A., 1985. Distribution of living coccolithophores in the California Current system, Southern California borderland. Mar. Micropaleontol. 9, 385–393.
Winter, A., Jordan, R.W., Roth, P.H., 1994. Biogeography of living Coccolithophores in ocean waters. In: Winter, A., Siesser, W.G. (Eds.), Coccolithophores. Cambridge University Press, London, pp. 161–178.
Wooster, W.S., Bakum, A., McLain, D.R., 1976. The seasonal upwelling cycle along the eastern boundary of the North Atlantic. J. Mar. Res. 34, 131–140.
Wright, A.K., Flower, B.P., 2002. Surface and deep ocean circulation in subpolar North Atlantic during the mid-Pleistocene revolution. Paleoceanography 17, 1068. http://dx.doi.org/10.1029/2002PA000782.
Wu, G., Yasuda, M.K., Berger, W.H., 1991. Late Pleistocene carbonate stratigraphy on Ontong–Java Plateau in the western equatorial Pacific. Mar. Geol. 99, 135–150.
Yin, Q.Z., Berger, A., 2012. Individual contribution of insolation and CO_2 to the interglacial climates of the past 800,000 years. Clim. Dyn. 38, 709–724.
Zahn, R., Schönfeld, J., Kudrass, H.R., Park, M.H., Erlenkeuser, H., Grootes, P., 1997. Thermohaline instability in the North Atlantic during meltwater events: Stable isotope and ice-rafted detritus records from Core SO75-26KL, Portuguese Margin. Paleoceanography 12, 696–710.
Ziveri, P., Thunell, R.C., Rio, D., 1995. Export production of coccolithophores in an upwelling region: results from San Pedro Basin, Southern California Borderlands. Mar. Micropaleontol. 24, 335–358.
Ziveri, P., Baumann, K.-H., Boeckel, B., Bollmann, J., Young, J., 2004. Biogeography of selected Holocene coccoliths in the Atlantic Ocean. In: Thierstein, H.R., Young, Y.R. (Eds.), Coccolithophores: From Molecular Processes to Global Impact. Springer, Berlin, pp. 403–428.